Development of Self-Nanomicellizing Solid Dispersion Loaded with Combination of Astaxanthin and Curcumin to Enhance Cytotoxic Effect Against HCT-116 Colon Cancer Cells

Project Facilitated by

College of Medicine and Public Health, Flinders University

05/02/2021

Written By: Hiral Desai

Acknowledgements

The year 2020 has been difficult for everyone due to the pandemic caused by Covid- 19. It was especially difficult for me being an international student and not being able to go home. During my education, my family in India was suffering from Covid- 19 along with some financial stress. One cannot help being home-sick during such times. I have been through mental, emotional, and financial stress. I was not able to get results for my preliminary tests for a long time and faced optimization challenges.

During this time, I had full support of my supervisor Associate Professor Munish Puri. From day one, he had been understanding of my circumstances and was very helpful. When he was made aware of my struggles, he got me all the assistance I needed to continue with my lab work. He was extremely patient with me. I may not have been an ideal student, but professor Munish always pushed me to be better, not just at my academic work but with my ethics at work. I am grateful and honoured to have had the chance to work under his guidance.

My co-supervisor, Professor Sanjay Garg at University of South Australia (UniSA), has been extremely supportive as well. He has been compassionate and understanding of my extreme circumstances. We had to work with tight deadlines, and he got me all the assistance and more, which I needed to finish my thesis. Even though I am not officially a student at UniSA, I got access to state of the art equipment and learn about all different kinds of techniques all thanks to him. He always tried to show me the reality of the situation and yet gave some important suggestions to carry out as much work as I can in the limited time I had because he was aware that I was eager to learn some key skills. I owe him a great debt of gratitude.

I am also extremely grateful to Dr Biju Balakrishnan (Flinders University) and Dr Ankit Parikh (UniSA). Both of them have imparted knowledge and taught me some important skills. They have

been of extreme help in the lab and also taught me to analyze the results. They also provided with their feedbacks and suggestions on the thesis. I would not have been able to finish my lab work without their help. I would also like to thank Dr. May Song, Nobuyuki Kawashima, and Franklin Afinjuomo (UniSA) for their time and assistance, and Kushari Burns, Lui Fei Tan, and Peng Su (Flinders University) for all their help, suggestions, and assistance in the lab.

Thanks to the whole staff of Medical Biotechnology Department (Flinders) and Clinical and Health Sciences Department (UniSA). I would like to take this opportunity to thank my batch mates Bunu Tamang and Simranjeet Kaur for their support, guidance and assistance in the lab, Tarandeep Kaur, Samuel Rollin, and Matthias Orchard for all the love and emotional support in difficult times. Lastly, I owe a huge debt of gratitude to my parents Siteshchandra Desai and Minaxi Desai without whom life would be impossible and my brothers Harsh Bardoli and Nikunj Bardoli without whom this journey at Flinders University would only have been a dream!

Contents

Contents

List of Abbreviations

5- FU- 5- Fluorouracil

AST- Astaxanthin

ATCC- American type cell culture

CAGR- Compound annual growth rate

CCA-1.1- Chemopreventive curcumin analogue

Conc^{n}- Concentration

COX-2- Cyclooxygenase-2

CUR- Curcumin

DMSO- Dimethylsulfoxide

DSC- Differential scanning calorimetry

ERBB- Erythroblastic leukaemia viral oncogene homologue

Erk/MAPK- Extracellular signal-regulated kinases/mitogen-activated protein kinases

FBS- Fetal bovine serum

FTIR- Fourier transform infrared spectroscopy

H. pluvialis- Heamatococcus pluvialis

HIF-1- Hypoxia-Inducible Factor (HIF)-1

iNOS- Inducible nitric oxide synthase

JAK-STAT- Janus kinases- signal transducer and activator of transcription proteins

MAPK- Mitogen-activated protein kinase

MAPK1- Mitogen-activated protein kinase 1

miRNA- microRNA

MMP1- Metalloproteinase 1

MMP2- Metalloproteinase 2

MMP9- Metalloproteinase 9

mtDNA- Mitochondrial DNA

mTOR- Mechanistic target of rapamycin

MTT- 3-(4,5-dimethylthiazol-2-yl)-2,5-diphenyltetrazolium bromide

NF-Kβ- Nuclear factor kappa light chain enhancer of activated B cells

p53- Tumor protein 53

PI3K-Akt- Phosphatidylinositol 3-kinase- protein kinase B

PLGA- poly lactic acid co glycolic acid

SEM- Scanning electron microscopy

SD- Solid dispersion

Sol- Soluplus

TNF- Tumor necrosis factor

TP53- Tumor protein 53

USD- US Dollars

VEGF- Vascular endothelial growth factor

List of Tables

List of Figures

Abstract

Carotenoid such as Astaxanthin (AST) and phenolic compound such as curcumin (CUR) possess anti-inflammatory, anti-oxidant, anti-cancer, anti-ageing, and anti-coagulant properties. However, both bioactives are poorly soluble in water and hence, all these properties as stated above cannot be exploited for therapeutic purposes at its full potential. In this study self-nanomicellizing solid dispersion (SD) of AST and CUR was investigated. Since both compounds possess anti-cancer activity, it was hypothesized that a combination of AST and CUR when provided in the form of a self-nanomicellizing solid dispersion it will have synergistic cytotoxic effect on colorectal cancer cell line (HCT-116).

This study developed self-nanomicellizing SD of AST and CUR to investigate its synergistic cytotoxic effect on HCT- 116 colon cancer cells. Solvent evaporation method was used to formulate the SDs for CUR. Whereas, AST was freeze-dried to obtain the SDs after solvent evaporation. Characterization of the SDs using different techniques such as FTIR, SEM, and DSC was carried out. Solubility, entrapment efficiency, and loading ability of the SDs were calculated by HPLC analysis. The cytotoxicity was measured by conducting the MTT assay after 48 h of treatment.

Self-nanomicellizing SD of AST had solubility of 3.67 µg/ml whereas CUR had solubility of 5285 µg/ml. The SD of the combination of AST and CUR had CUR within it with the solubility of 128 µg/ml, and AST with 2.85 µg/ml solubility. There was significant improvement in the solubility of the previously poorly soluble compound. The cytotoxic effect of SD of AST is 85% when dissolved in water and 51.4% when dissolved in DMSO, whereas for SD of CUR it is 85.1% and 92.2% when dissolved in water and DMSO respectively. As hypothesized, SD of the combination

of AST and CUR has synergistic cytotoxic effect of 89.9% and 98.1% when dissolved in water and DMSO and the p-value is 0.0081 (**, $p<0.05$) when compared against combination of free AST and CUR. In conclusion, the experimental results showed that the combination of CUR and AST using self-micellizing drug delivery system can reduce HCT-116 cell's viability, which could be considered as a promising complimentary treatment approach for colon cancer treatment.

Chapter 1 Introduction

1.1 Colon cancer

The failure in apoptosis which is programmed cell death of damaged or old cells leads to abnormal growth and continuous cell proliferation resulting in cancer (Karanam et al., 2020). Colorectal cancer is a malignant tumour in colon or rectum. It was reported that mutations or irregularity in the signalling pathway VEGF, HIF-1, ERBB, PI3K-Akt, MAPK, JAK-STAT, mTOR, TNF, p53, etc. can cause colorectal cancer (Wulandari et al., 2020).

In 2018, there were approximately 18.1 million new cases of cancer reported globally and 9.6 million people died of cancer globally (Ferlay et al., 2019). According to a recent report from the Cancer Australia, 2019, approximately 145,000 people were affected by cancer in Australia in 2019. It was estimated that approximately 15,494 new cases of colorectal cancer would be diagnosed in 2020 in Australia. This was 11% of the total cancer cases to be diagnosed in 2020. The estimated number of deaths due to colorectal cancer was 5322. It was also 11% of total cancer-related deaths in 2020 (Cancer Australia, 2020).

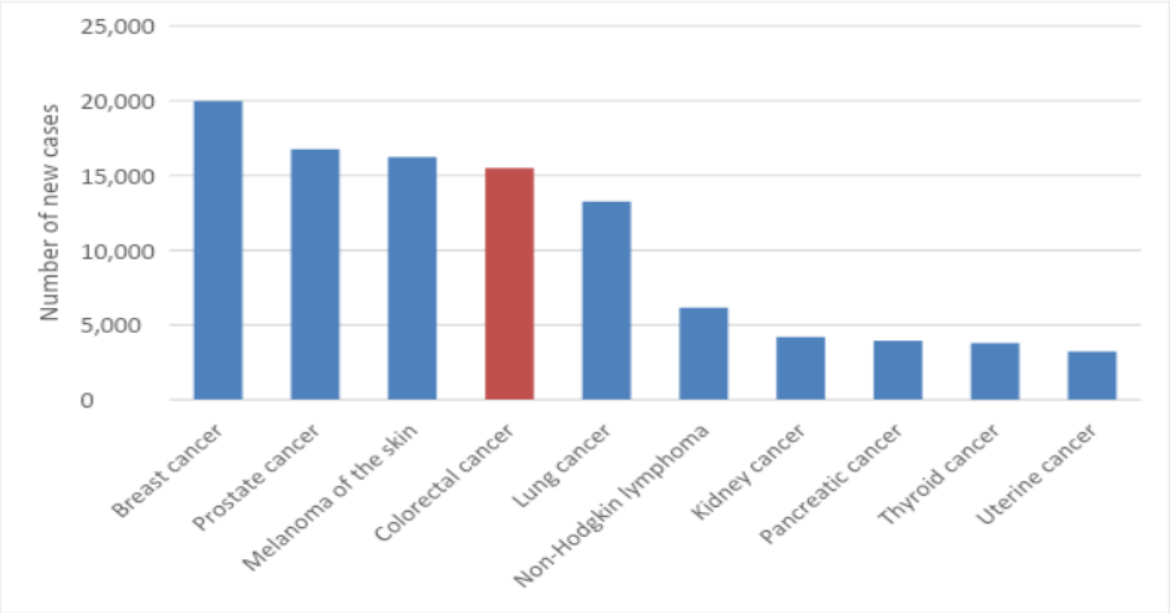

Figure 1.1 Estimate of most common cancers diagnosed in 2020 (Cancer Australia, 2020).

1.1.1 Current treatments and shortcomings

Different types of treatments have been developed depending on the type and stage of cancer a patient is suffering from. Current treatments include surgery, chemotherapy, anti-angiogenesis therapy, radiotherapy, and immunotherapy (Xiong et al., 2019). However, there are limitations to these treatments. Multidrug-resistant cancers, severe side effects, lack of target-specific drugs, the rapid spread of metastatic cancer, complications in normal tissue function, immunogenic response, low response, and acquired resistance towards treatment (Gao et al., 2019, Wirsdörfer et al., 2019) has resulted in controversies regarding the current therapeutical interventions.

Chemotherapeutic treatment kills cancerous cells or prevents its proliferation as well as prevents it from metastases. However, it is non-specific and does not only affect the cancer cells but affects the healthy cells as well. It causes inflammation which results in side effects like nausea, diarrhoea, hair loss, and sexual dysfunction as suggested by Abandansari et al., (2017). It also causes

depression in some cases and affects the general health and well-being of a patient (McFarland, 2019).

Immune cells can identify and kill cancer cells. However, cancer cells have developed a mechanism to evade the attack by immune cells (Tan et al., 2020). Bush and Noe; (2020) observed that the patient becomes unresponsive to the treatment due to resistance. Radiation therapy is often used in combination with chemotherapy. However, Münstedt et al., (2019) asserted it leads to numerous toxicities like oral mucositis which causes dose-limiting inflammation, ulcers in the oral cavity, pain, odynophagia, dysgeusia, dehydration, malnutrition, systemic infections which eventually results in dose reduction or discontinuation of the treatment.

Hence, it is important to come up with an alternative treatment to over-come all the toxicities, limitations, and efficacy issues of the current treatment. Nano-formulation of various bioactives, an alternative for treating cancer, has been used recently for treating stomach, breast, lung, urinary bladder, cervical, pancreatic, and colorectal cancer cells (Jayaprakasha et al., 2016; Liu et al., 2017; Doktorovova et al., 2018; Khan et al., 2018; Shanmugapriya et al., 2018; and Shen et al., 2019).

1.2 Issues and solution

A drug needs to cross various physiological barriers such as nasal mucous membrane, gastrointestinal barriers, skin, and blood-brain barrier (Leiva-Vega et al., 2020). While passing through these barriers the drug undergoes partial degradation (Zhang et al, 2016; and Yang et al., 2017). As a result, the drug becomes less effective and must be administered repeatedly which can be harmful to the patient.

Recent studies have shown that carotenoids (Miyashita et al., 2020) and flavonoids reported to have anti-inflammatory and antioxidants effects (Ajji et al., 2020). Based on their interesting antioxidant and anti-cancer activity, astaxanthin (AST) which is a β- carotenoid and curcumin (CUR) which is a phenolic compound were selected for this research. CUR has low aqueous solubility and poor bioavailability (Pathak et al., 2015). AST is also insoluble in water and has bioavailability issues. It is suspected that astaxanthin's strong lipophilic nature causes it to have less bioavailability (Zanoni et al., 2019).

Nanotechnology has been widely researched for drug delivery and its intervention enhanced bioavailability and biocompatibility. Nanoparticles result in controlled release of the drug, improves the stability of the bioactive compound, enhances cellular absorption of the drug, as well as protects the bioactive compound from degradation at various physiological barriers (Madhavi et al., 2018; De Matos et al., 2018; and Walia et al., 2019). Synthetic polymer can be used for nanomicelle formation of a bioactive compound which results in increased bioavailability of desired bioactive and makes the drug more effective.

1.3 Aim and hypothesis

Studies have revealed an individual anti-cancer effect of AST and CUR on colon cancer cells (See Table 2.1) however, both bioactive compounds have bioavailability issues. Solid dispersion of combination of AST and CUR could have more efficient and synergistic cytotoxic effect thus would promote solubility and enhance apoptosis in cancer cells.

It was hypothesized that a combination of AST and CUR when provided in the form of a self-nanomicellizing solid dispersion will have synergistic cytotoxic effect on colorectal cancer cell line (HCT-116). To test this hypothesis following objectives study were investigated:

- To develop solid dispersion of astaxanthin.
- To develop solid dispersion of curcumin.
- To develop solid dispersion of combination of astaxanthin and curcumin and its biochemical characterization following spectroscopy techniques.
- To test the functionality of all bioactive formulations against HCT- 116, a colon cancer cell line.

1.4 Significance

The use of bioactive compounds such as AST and CUR could reduce inflammation which is a common side effect of chemotherapy. This research will assist in assessing bioavailability of SD both AST and CUR as nanoparticles have proven to increase the bioavailability of both these compounds (Liu et al., 2019a, Liu et al., 2019b). It might be an alternative treatment for colon cancer which is one of the most prevalent types of cancer in Australia.

Chapter 2 Literature Review

2.1 Drugs and their side-effects

Doxorubicin is an anthracycline which is extracted from *Streptomyces peucetius*. It is used in the treatment of tumours and different types of cancer including breast, bile ducts, prostate, uterus, ovary, oesophagus, stomach and liver tumours, childhood solid tumours, osteosarcomas and soft tissue sarcomas, Kaposi's sarcoma, as well as acute myeloblastic and lymphoblastic leukaemia and Wilms tumour (Thorn et al., 2011).

It has several side effects which include and are not limited to acute nausea and vomiting, stomatitis, gastrointestinal disturbances, alopecia baldness, neurologic disturbances (hallucinations, vertigo, dizziness), cumulative cardiotoxicity and bone-marrow aplasia (Liu et al., 2006b, Hortobagyi, 1997). Doxorubicin is non-targeted and as a result, causes tissue necrosis. Normal mitochondrial function, proteins expression and lipid oxidation are hindered when it reacts with mitochondrial DNA (mtDNA) to form a product (Eder and Arriaga, 2006). It also showed toxicity to the brain, kidney, and liver depending on the dosage applied (Carvalho et al., 2009).

Paclitaxel (taxol) is derived from plant product isolated from the bark of the Pacific yew tree. It is mainly used against ovarian, breast, and non-small cell lung cancer. Some of the common side-effects include nausea and vomiting, diarrhoea, fatigue, headache, alterations in taste, and pain and erythema at the injection site (Rowinsky et al., 1990).

Its side-effects include hypersensitivity reaction, neurotoxicity, and cardiotoxicity. It causes myelosuppression which is a reduction in RBCs, WBCs, and platelet, hepatocytotoxicity resulting in elevated bilirubin, alkaline phosphatase, serum glutamic oxaloacetic transaminase (SGOT), and

serum glutamic pyruvic transaminase (SGPT), cardiotoxicity rarely resulting in an atrioventricular block, or ventricular tachycardia, mucositis, myalgias, alopecia also termed as hair loss, hypersensitivity reactions, neurological symptoms based on the dosage administered (Onetto et al., 1992; Rowinsky et al., 1992; and Walker, 1993).

Resveratrol is a polyphenol extracted from grape and other food groups. It has been used against colorectal cancer, hepatic cancer, and breast cancer. The most common toxicity related to resveratrol is abdominal pain, nausea, and flatulence in a dose-dependent manner (Cottart et al., 2014). It also causes nephrotoxicity, blood electrolyte changes, nasopharyngitis, erythematous rashes, elevated blood bilirubin or alanine transferase level, severe frontal headaches, myalgia of lower extremities, epididymitis, and dizziness (Cottart et al., 2010).

Hence, an alternative natural compound with high toxicity would be desirable. AST, global market is USD 1 billion (Astaxanthin Market Analysis Report, 2020), has been used for/as an anti-oxidant, cardiovascular health, anti-ageing, healthy skin, cosmetic, and eye, skin, joint, muscle and immune health (Ambati et al., 2014). Similarly, CUR (market share is USD 58.4 million with a CAGR of 12.7%) has applications in skincare including prevention of ringworm, eye infection, leech bites, sore skin, bruising, and swelling, as a cosmetic, potential therapeutic agent for the treatment of Alzheimer, coronary diseases, and cancer (Curcumin Market Analysis Report, 2020). Considering multiple applications and growing nutraceutical market, AST and CUR were selected as a compound of interest to formulate an anti-cancer drug.

2.2 Astaxanthin

2.2.1 Sources

AST, a β- carotenoid chemically known as (3,3′-dihydroxy-ß,ß'-carotene-4,4′-dione) is obtained from marine sources such as lobsters, salmons, shrimps, microalgae like *Haematococcus pluvialis* and *Xanthophyllomyces dendrorhous*, and marine bacteria like *Agrobacterium aurantiacum* (Faraone et al., 2020).

2.2.2 Chemical structure

AST is a xanthophyll as it contains carbon, hydrogen, and oxygen. It has 2 terminal rings which are connected by a polyene chain. There are 2 asymmetrical carbons anchored on the 3, 3’ positions of the β-ionone ring with a hydroxyl group (-OH) on each end of the molecule. If one hydroxyl groups reacts with a fatty acid, a mono-ester is formed, whereas a di-ester is formed if the hydroxyl group on both the ends reacts with fatty acids. It exists in stereoisomers, geometric isomers, free and esterified forms (Ambati et al., 2014). The molecular weight of AST is 596.8 g/mol.

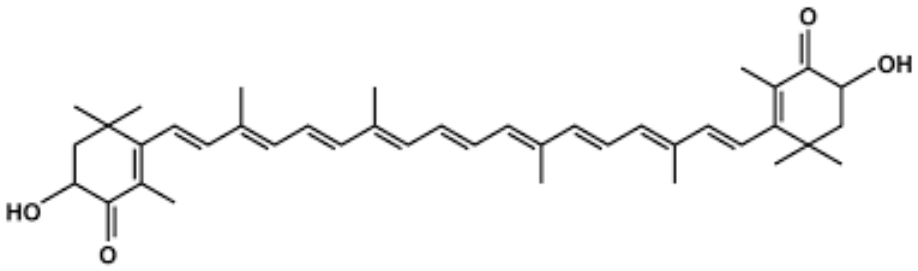

Figure 2.1 Chemical structure of AST (Astaxanthin structure, Pubchem).

2.2.3 Bioavailability

AST has low solubility in water and poor oral bioavailability due to extremely hydrophobic nature (Liu et al., 2019b). It is highly unstable and degrades during processing, storage, and digestion. It degrades under highly acidic pH condition, certain enzymes, oxygen, light, and certain food particles can also degrade it. Its bioavailability is less than 10% from raw vegetables.

Its bioavailability has been enhanced using fats. Its bioavailability and the anti-oxidant property has been increased using *Haematococcus pluvialis* biomass dispersed in oil (Rao et al., 2013). The increase in unsaturation degree of fatty acid resulted in an increase in bioavailability of AST (Yang et al., 2020). Enhancing the bioavailability of AST using fats is a complex process and hence lipid formulations which eventually formed micelles were used to overcome this complexity. When lipid formulation was used the bioavailability of AST increased by 3.7-fold. It had a half-life of 15.9 ± 5.3 h.

Emulsions have been used to increase the bioavailability of AST. A similar approach was used. The emulsion was prepared but the droplet size was reduced. It had enhanced half-life of 29.7 ± 7.4 h, 28.9 ± 5.4 h and 27.5 ± 6.6 h for nanosized and macro-sized emulsion and oil solution, respectively. The maximum concentration of AST observed in plasma for nanosized AST emulsion was 698.7 ± 38.7 ng/mL, macro-sized AST emulsion was 465.1 ± 43.0 ng/mL, and oil solution was 313.3 ± 12.9 ng/mL (Affandi et al., 2012).

AST nanoparticles have also been used to enhance the solubility of AST. AST loaded chitosan-coated PLGA nanoparticles with the size of 150 nm were prepared. It had an encapsulation efficiency of approximately 93.5%. It got encapsulated in an amorphous state which increases

solubility and bioavailability of a compound. PLGA (poly (lactic-co-glycolic) acid) is a biodegradable polypeptide chain often used to produce nanoparticle (Liu et al., 2019a).

2.2.4 Biological application

AST has antioxidant, anti-inflammatory effects, and can target cancer-causing abnormal signalling pathways that lead to apoptosis (Faraone et al., 2020). It has anti-cancer effects against colorectal cancer, prostate cancer, melanoma, breast cancer, lung cancer, hepatic cancer etc. (Faraone et al., 2020). It can cause apoptosis by activating natural killer cells, interleukin, protein kinase B, and tumour necrosis factor (See Table 2.1).

A study investigated concentration of 20, 40, 60, and 80 µM of AST used against breast cancer cells and found to have an apoptotic effect against SKBR3 cell line (Kim et al., 2020). They aimed to identify the mechanism through which AST causes cell death as it also has an anti-oxidant effect and could be killing cells due to reactive oxygen species. However, they found that AST blocked cell cycle progression at G_0/G_1, suppressed proliferation dose-dependently, and induced apoptosis of the cells. It was found that a concentration of 5, 25, 50, 100, 125 µg/ml of AST was efficient for inhibited growth, migration, and invasion of melanoma A375 and A2058 cells (Chen et al., 2017). AST treatment inhibited expressions of MMP-1, MMP -2 and MMP -9 in a dose-dependent manner. MMP are a class of matrix metalloproteinase enzyme which plays a role in the breakdown of the extracellular matrix. AST blocks both upstream kinases Erk/MAPK and PI-3K/Akt and their downstream signalling pathways NF-κB and Wnt/β-catenin thus causing apoptosis. It causes inhibition of phosphorylation of transcription factors and kinases as evident from gene expression and docking analysis. As a result, caspase-mediated apoptosis occurs (Kavitha et al., 2013).

In a study, a concentration of 4, 6, 8, 10, 12, 14, and 16 μM was used for 24, 48, and 72 hours against HCT116 & HT29 which are colon cancer cell lines (Liu et al., 2016b). IC50 values of AST after 72 hours of treatment were 7.42, 7.48, and 7.51 μM in HCT116. The inhibition on the cancer cells was associated with extensive cell cycle arrest and apoptosis caused by S, R, and M stereoisomers of AST as a result of modulation of oncogenic signalling proteins. Group of researchers nano-encapsulated AST using potato protein (Edelman et al., 2019). When they evaluated bioaccessibility, potato protein degradation, and AST retention through simulated digestion models they found that AST nano-encapsulated with potato protein had 80% bioaccessibility for intestinal absorption, lower potato protein degradation which meant more protection of AST compound, and 78% AST retention. It had 7.5-fold higher bioavailability as compared to free AST.

Image removed due to copyright restriction.
Original available online from the publisher:
https://www.sciencedirect.com/science/article/pii/S0304416513002286?via%3Dihub#f0040

Figure 2.2 Metabolic effects of astaxanthin causing apoptosis (Kavitha et al., 2013).

2.3 Curcumin

2.3.1 Sources

CUR is chemically (diferuloylmethane)-(1,7-bis (4-hydroxy-3-methoxyphenyl)-1, 6-hepadiene-3,5-dione) which is a polyphenol extracted from *Curcuma longa* also known as Turmeric (Liu et al., 2017).

2.3.2 Chemical structure

CUR is found in nature in bis-α, β-unsaturated β-diketone. It demonstrates a keto-enol tautomerism in which case it is present as different conformer based on the environment namely solvent and pH (Priyadarsini, 2009). In acidic and neutral medium it is present as keto form, whereas in alkaline media it exists in an enol form. The molecular weight of CUR is 368.38 g/mol.

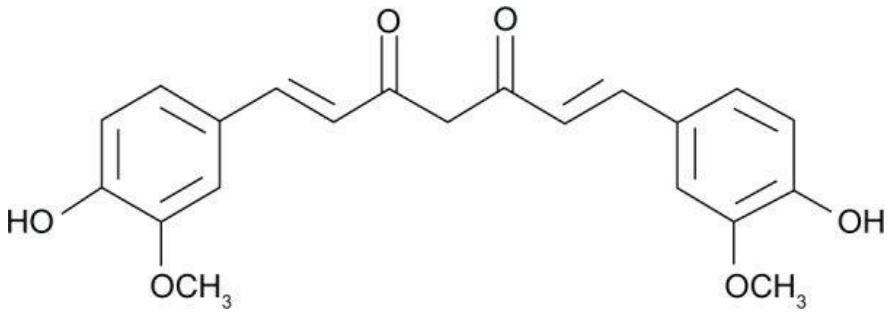

Figure 2.3 Chemical structure of CUR (Farazuddin et al., 2014).

2.3.3 Bioavailability

Low solubility in water leads to poor absorption of CUR in the gastrointestinal tract (Purpura et al., 2018). It's hydrophobic in nature and hence possesses low bioavailability. It was reported that

CUR had approximately 1% bioavailability after oral administration in Wistar rats (Yang et al., 2007). Rapid metabolism is also a reason for poor bioavailability.

Phospholipid complexes can be used to increase the bioavailability and absorption of CUR as it is amphiphilic in nature and can increase both water and lipid solubility. It was found in a study that CUR-phospholipid complex when administered orally in a male rat at a concentration of 100 mg/kg, the maximum level of CUR-phospholipid complex found in plasma was 600 ng/ml as compared to free CUR which was only 267 ng/ml (Liu et al., 2006a). The CUR absorption increased by 1.5 folds in male rats in that study.

Microemulsions are dispersions consisting of an oil phase, water phase, surfactant, and co-surfactant. Microemulsions are easy to prepare, have thermodynamic stability, high solubilization capability, provide protection from degradation, hydrolysis, and oxidation. Parallel artificial membrane permeability assay was used in a study to determine the oral absorption of CUR microemulsion *in- vitro*. The optimized microemulsion had enhanced solubility of 14.57 mg/ml and the artificial membrane was permeable to 17.44 μg and 120.12 μg after 6 h and 24 h respectively. The solubility increased 10,000 folds in this study (Bergonzi et al., 2014).

Polymeric micelles are amphiphilic blocks of copolymer that spontaneously form micelles whose size ranges from 20 to 100 nm. A group of scientists made a mixture of micelles composed of Pluronics P123 and F68 at the ratio of 2.05:1 using central composite design for optimization. They found the loading efficiency and capacity of CUR was approximately 87% and 7% respectively. The concentration of CUR used to form micellar solution was 3.02 mg/ml whereas for free CUR the solubility is 11 ng/ml. so the solubility increased 27,500 folds. The size of the micelles was approximately 68.2 nm (Liu et al., 2016a).

2.3.4 Biological application

A recent review suggested that CUR has anti-ageing, anti-cancer, anti-inflammatory, anti-oxidant, and anti-coagulant effects (McCubrey et al., 2017). CUR in doses of 2.5-10 μmolar has anti-cancer effects against brain cancer, cervical cancer, prostate cancer, oesophagal cancer, bladder cancer, colorectal cancer, head and neck cancer, lung cancer (McCubrey et al., 2017). CUR can regulate miRNA expression to cause apoptosis via natural killer cells, caspases, or protein kinase B as shown in Table 1.1 Despite CUR being effective in killing cancer cells, its low bioavailability limits its use as a drug at higher doses.

It was observed that the bioavailability issue related to CUR can be solved by making solid nanoparticles of CUR (Sun et al., 2013). They found the bioavailability to increase by 125%. (Slika et al., 2020) found in their study that CUR combined with polyallylamine hydrochloride triggered cytotoxic effect against colorectal cancer cells in mice when stimulation was provided in presence of dimethylhydrazine. It was observed that its ability to suppress cancer cell proliferation by inhibiting COX-2 and iNOS enzymes. A detailed bioinformatic study was investigated to find out the target genes of CCA-1.1 (Wulandari et al., 2020). Three target genes with the help of Kaplan Meier survival plots namely TP53, MAPK1, and ERBB2 which had significant implications on colon cancer cell proliferation were studied.

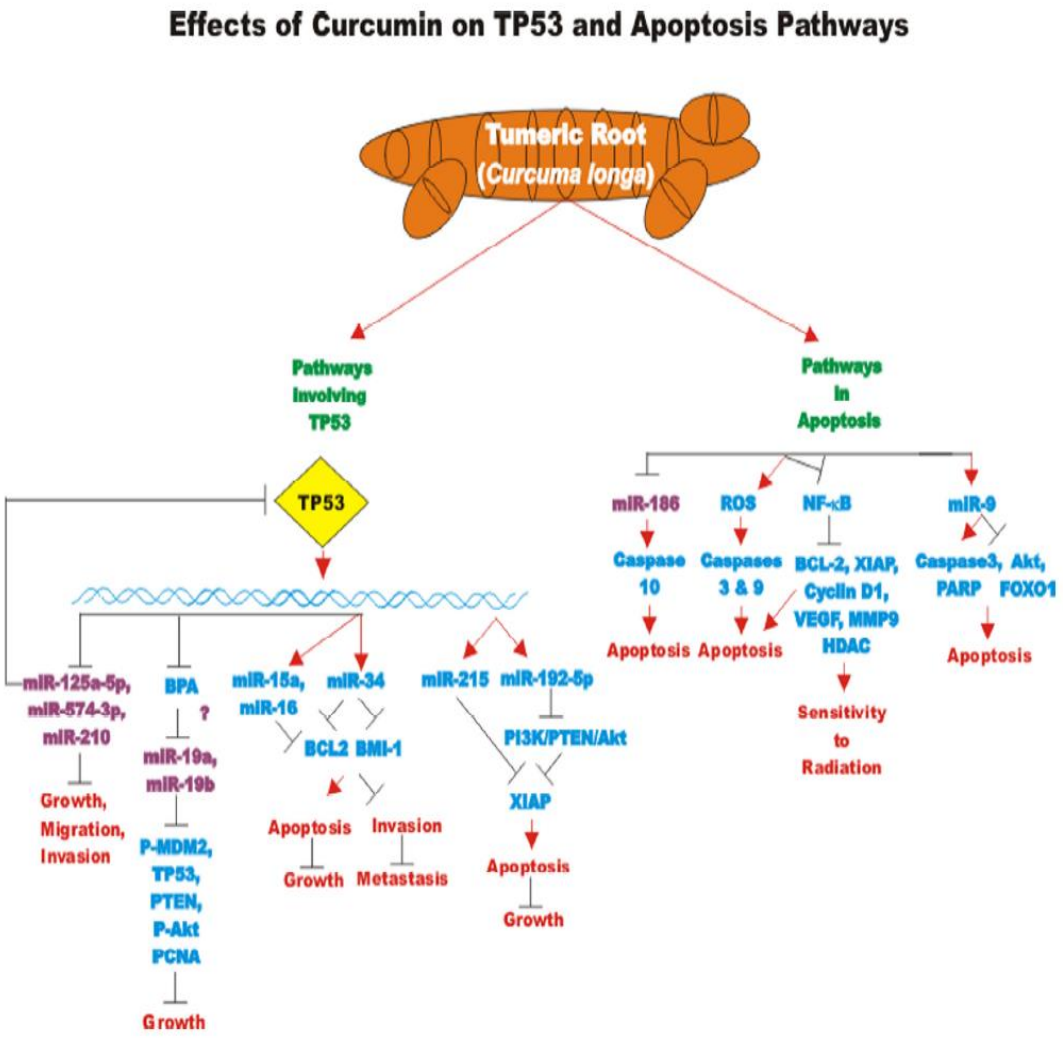

Figure 2.4 Effect of CUR on tp53 and apoptosis pathways resulting in cell death (McCubrey et al., 2017).

A combination of CUR and 5- Fluorouracil was investigated. They found IC50 values of CUR and 5-FU to be 20 µM and 5 µM respectively (Shakibaei et al., 2013). As stated in this study 5-FU and other chemotherapeutic agents stimulates transcription factor NF-Kβ and Src which induces survival, proliferation, invasion, and metastasis of colon cancer cells which eventually results in the development of drug resistance. CUR prevents this from happening by targeting both NF-kβ

and Src pathways, thus promoting apoptosis of colon cancer cells. In a recent study CUR emulsomes were used which has characteristics of both a liposome and an emulsion (Bolat et al., 2020). They used a concentration of 5 to 50 μM and found emulsomes to have controlled release of the drug. It released only 40% of the CUR in 72 hours. They found the highest cell inhibition with 50% cell viability at a concentration of 25 μM after 48 and 72 hours.

2.4 Soluplus

2.4.1 Chemical structure

Soluplus® (SOL) is an amphiphilic polyvinyl caprolactam–polyvinyl acetate–polyethylene glycol grafted copolymer. It can be used to formulate solid dispersions (SD), nano-suspension, and micelles by spray drying, hot-melt extrusion, and wet granulation. It appears like white or yellowish granular powder. SOL is widely used to increase the bioavailability and stability of hydrophobic compounds. The polymer has a hydrophilic and a hydrophobic segment which interacts with the hydrophobic drug and forms a micelle (Kamal et al., 2020).

2.4.2 Biological applications

Lopinavir is classified as a class IV biopharmaceutical drug with low bioavailability and poor permeability. Lopinavir in a SOL matrix had 1.7 fold more bioavailability as compared to VA-64 and 3.7 fold more than that of lopinavir crystals itself. After incorporating verapamil with lopinavir the permeability increased 2 fold. It was concluded that SOL matrix improved bioavailability by 3 mechanisms namely, hydrogen bonding with lopinavir, micelle formation in water, and P-glycoprotein (enzyme inhibitor) inhibition *in- vivo* (Zi et al., 2019).

It was observed that CUR dissolved faster in SOL as opposed to Poloxamer (Homayouni et al., 2019). The particle size with SOL was also smaller which was 258- 459 nm as compared to that of Poloxamer which was 311- 339 nm. However, the dissolution rate of CUR in presence of both polymers accelerated with the increase in the amount of the polymer.

A SD of resveratrol with SOL and surfactants such as Gelucire and poloxamer 407 was prepared (Vasconcelos et al., 2021). It was observed that resveratrol SOL complex had 2 fold more solubility in the absence of these 2 surfactants whereas it had 8 fold higher solubility in the presence of both the surfactants. At a concentration of 15%, Poloxamer higher solubility was reported as compared to 5%, whereas Gelucire did not exhibit a statistically significant increase in solubility in either of the concentration at pH 1.2 and 6.8. The formulation with 15% Poloxamer was considered ideal as it had higher dissolution under acidic conditions, higher absorption, and higher positive response to the treatment from patients.

Based on a study, it was found that CUR forms microemulsion of approximately 54.33 nm in size and has a low polydispersity index (PDI) of approximately 0.18 which suggests the uniform distribution of CUR which is due to emulsification properties of SOL (Kamal et al., 2020). It had an entrapment efficiency of 93.3%. They used spray drying method for the formation of solid self-emulsifying drug delivery system (SEDDS) with SOL and neusilin; compared the SDs formed by both and concluded SOL to be a better carrier for SEDDS. When compressed into tablet form, CUR had controlled release over 24 hours with SOL. Both these studies suggested that apart from emulsification, SOL also provided stabilization to CUR. SOL has not yet been used as a carrier of AST which adds to the novelty of this research.

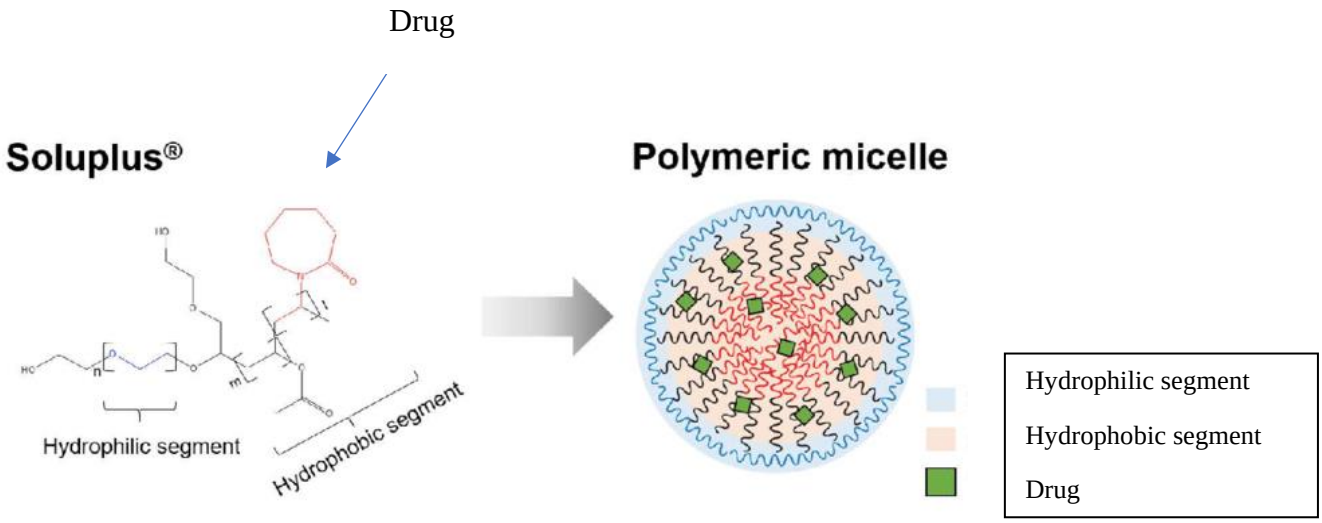

Figure 2.5 Chemical structure of SOL (Noh et al., 2018).

Table 2.1 *In- vitro* studies supporting the use of bioactives such as AST and CUR in different forms, sizes, and concentration against various cancer cell lines.

Compound	**Source**	**Form**	**Size**	**Conc^{n}**	***In- Vitro* Study**	**References**
AST	*H. pluvialis*	*H. pluvialis* extract			Hepatic cancer, Colorectal cancer,	Shanmugapriya et al., 2019
					Lung cancer,	
					Skin cancer	
		NanoParticle	106-220 nm	25µg/mL	Stomach gastric cancer, breast cancer	
	Blakeslea trispora	Nanoparticle	189-216 nm and	0.83-1.65 mg/g	Cervical cancer, Colorectal cancer,	Shanmugapriya et al., 2018

			106-213 nm		Urinary bladder cancer, Pancreatic cancer	
	Blakeslea trispora	Nano particle	190-285 nm	25mg/100L	Colorectal cancer	Shen et al., 2019
CUR	*Curcuma longa*	*Curcuma longa* (Turmeric) powder			Lung cancer	Liu et al., 2017
	Curcuma longa	Nanoparticle			Breast cancer, Lung cancer	Khan et al., 2018
	Curcuma longa	Nano particle	185-236 nm	16.85-30.90 µM	Colon cancer	Jayaprakasha et al., 2016
	Curcuma longa	Nano particle	165-289 nm	2.7 µM	Brest cancer	Doktorovova et al., 2018

2.5 Self-nanomicellisation

The global polymeric dispersion market share is estimated to grow from USD 7.48 billion in 2020 to USD 11.7 billion with a compound annual growth rate above 8.4% (Market Data Forecast, 2020). As mentioned above several approaches have been taken to increase the bioavailability of both AST and CUR. However, entrapping the compound in a micelle seems to be the best approach as it increases the bioavailability of both AST and CUR by approximately 3.7 and 27,500 folds (Liu et al., 2016a). Hence, the method of preparing self- nanomicellizing SDs was chosen for this study.

Figure 2.6 Drug entrapped within polymer resulting in SD formation (Vaka et al., 2014).

Chapter 3 Materials and Methods

3.1 Materials

3.1.1 Chemicals and buffers

Astaxanthin (97% purity) extracted from *Blakeslea trispora* was purchased (costing AUD 145 per 50 mg, Sigma Aldrich). Curcumin (66% purity) extracted from *Curcuma longa* was purchased (costing AUD 101 for 10 g, Sigma Aldrich) (Sigma Aldrich, St. Louis, MO, USA). SOL was used for the formation of SD. SOL was gifted by UniSA (Australia). SOL is the carrier whereas AST and CUR are the bioactives to be micellized**.** Trypsin EDTA, Phosphate buffer saline (PBS), MTT, and DMSO were purchased from Sigma Aldrich. Citric acid, Sodium hydroxide, Acetonitrile, HCl were obtained from Chem Supply.

3.1.2 Media and cell line

Colon cancer cell line HCT-116 was pre-established and was obtained from Flinders Medical Centre (Adelaide, Australia). McCoy media, Fetal bovine serum (10% FBS), Penicillin/streptomycin (1%), and Glutamax^{TM} (1%) were purchased from Sigma Aldrich.

3.1.3 Instruments

Instruments like rotovap (Rotavapor R210 BUCHI Switzerland), HPLC (UFLC XR SHIMADZU, Scientific instrument, Japan), orbital shaker (Innova 2300, Platform shaker), magnetic stirrer (CH2090-001 IEC, Australia), weighing balance (SB12001, Mettler toledo), vortex mixer (Ratek vortex mixer, Adelab scientific, Australia), freeze dryer (Labconco 77540, USA), centrifuge (Centrifuge 5804, Eppendorf, Germany), centrifuge (Allegra X12R, Beckman Coulter, USA),

centrifuge (Select spin21 Adelab Scientific, Australia), sonicator (SONICS Vira cell^{TM}), sonicator (5510 Branson, USA), water bath (Ratek temperature control, Adelab Scientific, Australia), -80 °C refrigerator (MDF -74V, Panasonic, Japan), FTIR spectrometer (PerkinElmer Spectrum 400 spectrometer, PerkinElmer, USA), differential scanning calorimetry (TA Instruments Discovery model 250, USA), SEM (Zeiss Microscopy Merlin with GEMINI II column, Germany), incubator (Forma 371 Steri Cycle Incubator, Thermo Scientific, USA), biosafety cabinet class II (N4425-6005, Nuaire, United Kingdom), Omega plate reader Ω (FLUOstar Omega, BMG Labtech, Germany), inverted microscope (AE2000, Motic, Germany), 96 well cell culture plates (Corning Costar®), micropipette, disposable pipette tips, pipette gun, and glass pipettes were used.

3.2 Methods

3.2.1 HPLC analysis of AST and CUR

AST and CUR's qualitative analysis was done using high performance liquid chromatography (HPLC). The Shimadzu HPLC system with a photodiode array detector was used for bioactive AST's and CUR's analysis. HPLC technique was used to ensure that both AST and CUR formed SDs. HPLC was conducted at 423 nm using a C18 reversed-phase column (250mm x 4.6mm x 0.005mm). Before sample injection, the column was equilibrated for 10 min with mobile phase consisting of acetonitrile (65% v/v) and citric acid buffer (35% v/v, pH=3) for CUR at a flow rate of 1 ml/min (Parikh et al., 2018). The retention time of CUR was 2.7 minutes. Whereas for AST, mobile phase A comprised of methanol, ethyl acetate, and water in the ratio of 88:10:2 and mobile phase B comprised of methanol, ethyl acetate, and water in the ratio of 48:50:2 respectively where absorption was detected at 450 nm wavelength using the same column. The flow rate was maintained at 1 ml/ minute (Singh et al., 2013). The retention time of AST was 2.9 minutes. The

SD with a combination of AST and CUR was run following HPLC methods to confirm the presence of both the compounds. All the formulations were centrifuged before carrying out HPLC to ensure there were no particles. The calibration curve for standard AST (varying concentration 25, 50, 100 µg/ml) and CUR (20, 40, 60, 80, 100 µg/ml) were prepared for identification and quantification of each sample. All samples were syringe filtered (0.22 um) prior to HPLC analysis of the samples.

3.2.2 Preparation of nano micelles

3.2.2.1 Solid dispersion of CUR

In order to prepare CUR SD with the ratio of 1:3, 1:6, and 1:9 with SOL 1 g CUR and 3 g SOL, 400 mg CUR and 2.4 g SOL, and 500 mg CUR and 4.5 g SOL respectively were used. SOL was dissolved in ethanol and a clear solution was obtained. Once the clear solution was obtained, CUR was added to it. It was ensured that no suspended particle remained in the solution. The ethanol from this clear mixture was allowed to evaporate for 1 h at 55 °C with the help of a Rotovap (Rotovapor, model R-210) to obtain the SD of the drug in powder form with the desired ratio (Parikh et al., 2018).

3.2.2.2 Solid dispersion of AST

AST stock solution (10 mg/ml) was prepared in ethanol. SOL was dissolved in water at a concentration of 10 mg/ml. After mixing 30 mg/ml of AST solution with 90, 180, and 270 mg/ml of SOL solution with the help of a magnetic stirrer for 1 h binary dispersions of different ratios (1:3, 1:6, 1:9) were obtained. The mixture was heated up in a water-bath at 50 °C for 15 minutes. The SD was allowed to cool at room temperature for 30 minutes and centrifuged at 10,000 rpm at

4 °C for 10 min to separate the precipitated AST. Before freeze-drying, solutions were frozen at -80°C for at least 6 h and then subjected to lyophilization using lyophilization chamber Labconco 77540 for at least 48 h. The formulation was stored at -20°C for further analysis (Lim et al., 2015).

3.2.2.3 Solid dispersion of AST and CUR

The combination (AST and CUR) was prepared in an AST to CUR ratio of 1:1, whereas the drug to carrier ratio was 1:9. So, 10 mg/ml stock of both AST and CUR was prepared in ethanol. AST and CUR were taken in the amount of 25 mg/ml and mixed with 225 mg/ml of SOL whose stock is prepared in water. Further, the freeze-drying method used for preparing the SD was the same as that of preparation method of SD of AST.

3.2.3 Entrapment efficiency and loading ability

Approximately 5, 7,10 and 10 mg of SD of CUR and SD of combination of AST and CUR in the ratio of 1:3, 1:6, 1:9 and 1:9 respectively was weighed and dissolved in 1 ml acetonitrile. Similarly, 10 mg of SD of AST and SD of AST and CUR in the ratio of 1:3, 1:6, 1:9 and 1:9 respectively was dissolved in mobile phase B. The sample was filtered through 0.45-µm polyvinyl difluoride syringe filter and analyzed by HPLC method. The loading ability of SD was calculated based on the weight ratio of CUR to SOL, AST to SOL, AST and CUR to SOL and encapsulation efficiency with the determination of loaded CUR, AST, AST and CUR in SD after preparation from initial amount (Parikh et al., 2018).

$$\text{Encapsulation efficiency (\%)} = \frac{Amount\ Of\ Drug}{Total\ amount\ of\ drug\ in\ the\ formulation}\ X\ 100$$

$$\text{Loading Ability (\%)} = \frac{Encapsulation\ Efficiency}{Total\ amount\ of\ carrier}\ X\ 100$$

3.2.4 Solubility tests

The method of HPLC for CUR required 1:3, 1:6, and 1:9 CUR SDs respectively dissolved in 20 ml of water and 100 mg SD containing AST and CUR (1:9) dissolved in 2 ml water to determine the amount of CUR in the SDs, while for AST 1:3, 1:6, and 1:9 AST SDs, and 10 mg of SD with the combination of AST and CUR (1:9) were dissolved in 2 ml of water and kept in a shaker for 24 h at 37 °C, 19 rpm. HPLC analysis was carried out after centrifugation to eliminate any particle to determine the solubility of CUR and AST (Parikh et al., 2018).

3.2.5 Characterization of the formulation

3.2.5.1 FTIR

PerkinElmer Spectrum 400 spectrometer which was connected to an attenuated total reflectance (ATR, top-plate type) (PerkinElmer) by traditional potassium bromide pellet method was used to record the FT-IR spectra. Approximately 2–4 mg of samples containing AST control, AST SD, CUR control, CUR SD, and combination of AST and CUR SD were taken for FTIR analysis. The range of 400–4000 cm^{-1} at a resolution of 2 cm^{-1} was used to scan each sample.

3.2.5.2 Differential scanning calorimetry

Differential scanning calorimetry was performed using differential scanning calorimetry (TA Instruments Discovery, model 250) to analyze the thermal behaviour of AST, CUR, SOL, AST SD, CUR SD, and AST and CUR combined SD. After weighing approximately 3–4 mg of every sample, it was placed in the aluminium crucible. A blank was set up by using an empty crucible.

The thermograms were obtained over the temperature range from 25 to 250 °C at the heating rate of 10 °C/min under nitrogen gas (50 mL/min).

3.2.5.3 Scanning electron microscopy (SEM)

The morphology of AST, CUR, SOL, AST SD, CUR SD, and AST and CUR SD (mixture) was observed using scanning electron microscopy. The samples were mounted on scanning electron microscopy stub using conductive double-sided adhesive tape prior to analysis. The morphological characteristics were studied using ultra-high resolution secondary electron microscopy (Zeiss Microscopy Merlin with GEMINI II column). The electron images were obtained by operating a microscope at 0.1- 0.5k V.

3.2.6 Cell culture

HCT-116 (ATCC®- CCL-247^{TM}) cells procured from ATCC were maintained at Medical Biotechnology Department and were grown in McCoy's media (M9309) containing 10% FBS, 1% Penicillin/streptomycin, and 1% Glutamax®. Once the cells reached 80% confluence the cells were sub-cultured according to standard protocol rinsed with 5 ml 1X PBS, and then 1 ml of 1X Trypsin was added for detachment and kept in the incubator at 37°C for 5-10 minutes. The T25 flasks were observed under an inverted microscope to check detachment of cells. During this process, cells should not be agitated, or clusters will be formed. After cells got detached trypsin was neutralized by addition of media which is 2 times more than the amount of trypsin added and pipetted in and out multiple times to complete detachment. This solution was centrifuged at 250x g for 5 minutes, the supernatant was discarded, and the pellet was resuspended with 5 ml of growth media. Cells were counted with the help of a hemocytometer and were seeded at a cell density of 5 X 10^4 cells per well. Resuspended cells were provided with fresh media in a ratio of 1:6 (1 part

sub-cultured cells, 6 part fresh media). Cells were incubated at 37 °C with 95% air and 5% CO_2 in an incubator.

Cell Density= (N/4) X 10 X 10^4 cells/ml

3.2.7 Cytotoxic assay

MTT assay was conducted to measure the cytotoxicity of the bioactive compounds and the novel formulation on colon cancer cells (Mosmann, 1983). HCT-116 cells at a density of 5000 cells per well were transferred to each well of a 96 well plate and then incubated in an incubator at 37 °C and 5% CO_2. Cells were treated with 5- Fluorouracil as a positive control at a concentration of 0.01, 0.1, 1, 10, 100 µM/ml. Based on the literature survey the concentration of free AST and CUR used was 3.125, 6.25, 12.5, 25, 50 µg/ml in triplicate. A similar concentration of 3.125, 6.25, 12.5, 25, 50 µg/ml in triplicate was used with the combination of AST and CUR. The cell viability was accessed with MTT (5mg/ ml) dye and IC50 value of AST and CUR were calculated with the help of non-linear regression dose inhibition function of GraphPad Prism software. A range of concentration of 3.125, 6.25, 12.5, 25, 50 µg/ml for SD of AST, 3.125, 6.25, 12.5, 25, 50 µg/ml for SD of CUR, and 3.125, 6.25, 12.5, 25, 50 µg/ml SD combination of AST and CUR was used. The free drug dissolved in water and DMSO was considered a control for the assay whereas the micellised drug prepared with polymer dissolved in water and DMSO was treatment. The stock solutions were sonicated to dissolve the drug for 30 minutes at high temperature before treatment.

After incubating the cells with free AST, free CUR, the combination of free AST and CUR, SD of AST, SD of CUR, the combination of equal concentration of SD of AST and SD of CUR, and a SD of the combination of AST and CUR for 48 h at different concentrations in a carbon dioxide incubator, the plates were washed with 1X PBS. MTT assay was then performed by adding 10 µL

of MTT (5 mg/ml) in each well and incubating for 4 hours. After the formation of formazan crystals addition of 50 µL DMSO was done to solubilize them and after 10 minutes of incubation optical density at 570 nm was measured by transferring the plates to an Omega plate reader (FLUOstar Omega, BMG lab). The blank values were reduced from the readings and percent live cells were calculated by dividing the blank reduced OD of treatment wells by blank reduced control wells. Percent of dead cells was calculated by reducing this value from 100.

3.2.8 Statistical analysis

A non-linear regression analysis was performed with the help of built-in IC50 function of GraphPad Prism version 9.0. The IC50 values were determined for each new compound against HCT-116 cells. Student's *T- test* function of Prism Graphpad was used to determine statistical significance of the treatments compared to each other. The level of significance was $p<0.05$.

Chapter 4 Results

4.1 Solubility

In the case of AST, the HPLC chromatogram exhibited 3.67 µg/ml of AST got solubilized in of water where the sample had the highest concentration of carrier (1:9). Similarly, for CUR, the sample with 1:9 ratio of drug to polymer was the most desirable formulation. HPLC chromatogram showed 5285.5 µg/ml of CUR was soluble in water. In comparison, the 1:3 and 1:6 SDs with AST and CUR respectively, only showed 0.29 and 3.45 µg/ml of AST, 24.4 and 1860.2 µg/ml of CUR were water-soluble. The solubility of the combination of AST and CUR formulation with water and 2.85 µg/ml of SD of CUR was detected by CUR's method of HPLC as well as 128.03 µg/ml of SD of AST was detected by AST's method respectively.

4.2 Entrapment efficiency and loading ability

The entrapment efficiency was 15.31% (w/w) and 95.6% (w/w) for AST and CUR's SD respectively. Approximately 1.7% (w/w) was loading ability of AST where the SD's ratio was 1:9; whereas 10.62% (w/w) was loading ability of CUR in SD with the ratio of 1:9. Meanwhile, 10.28% (w/w) and 1.40% (w/w) was loading ability of AST and CUR in the SD with AST and CUR combination respectively.

Table 4.1 Solubility, solubility increment (fold), entrapment efficiency, and loading ability of SD of AST, CUR, and combination of AST and CUR when different ratio of drug to the carrier are used.

Sample	Solubility (µg/mL)	Solubility Increment (Fold)	Entrapment Efficiency (%)	Loading ability (%)
CUR				
CUR	0.54	1		
CUR SD 1:3	24.4	45.18	48.26	16.08
CUR SD 1:6	1860.2	3444.81	70.47	11.74
CUR SD 1:9	5285.5	9787.96	95.60	10.62
Combination SD 1:9	128.03	237.09	12.67	1.40
AST				
AST	0.025	1		
AST SD 1:3	0.29	11.6	0.9124	0.30
AST SD 1:6	3.45	138	6.46	1.07
AST SD 1:9	3.67	146.8	15.31	1.70
Combination SD 1:9	2.85	114	92.55	10.28

4.3 Characterization of the formulation

4.3.1 FTIR

A distinct peak is observed at 3512, 1602, 1627, 1507, 1428, 1274, and 1153 cm $^{-1}$ with CUR as the control sample. Similarly, peaks are observed at 2927, 2865, 1729, 1624, and 1238 cm $^{-1}$ with CUR SD. Peaks 3490, 1649, 1549, 1314, 1278, and 975 cm $^{-1}$ were detected in AST control. Peak broadening from 3269 to 3647 cm $^{-1}$, and signals at 1728,1609,1446, and 1241 cm $^{-1}$ were obtained in case of AST SD. The peaks for SD of the combination of AST and CUR are 3616, 3295, 2927, 2850, 1731, 1624, 1238 cm $^{-1}$.

4.3.2 Differential scanning calorimetry

The peak for T_m of CUR is 173.34 °C, CUR SD is 81.16 °C, AST is 223.67 °C, AST SD is 187.29 °C, and SD of the combination of AST and CUR is 152.99 °C. There is an endothermic shift observed in SDs.

4.3.3 SEM

Free CUR appeared as large aggregates of smaller particles. There was no uniform size distribution. However, when it was uniformly distributed in SOL, flat uniform-sized particles were formed in CUR SD formulation. Free AST has extremely small-sized particles which are densely clumped together. AST SD also gave rise to an amorphous structure as can be observed in SEM. The combination of micellized AST and CUR was observed to have formed a thin film-like structure.

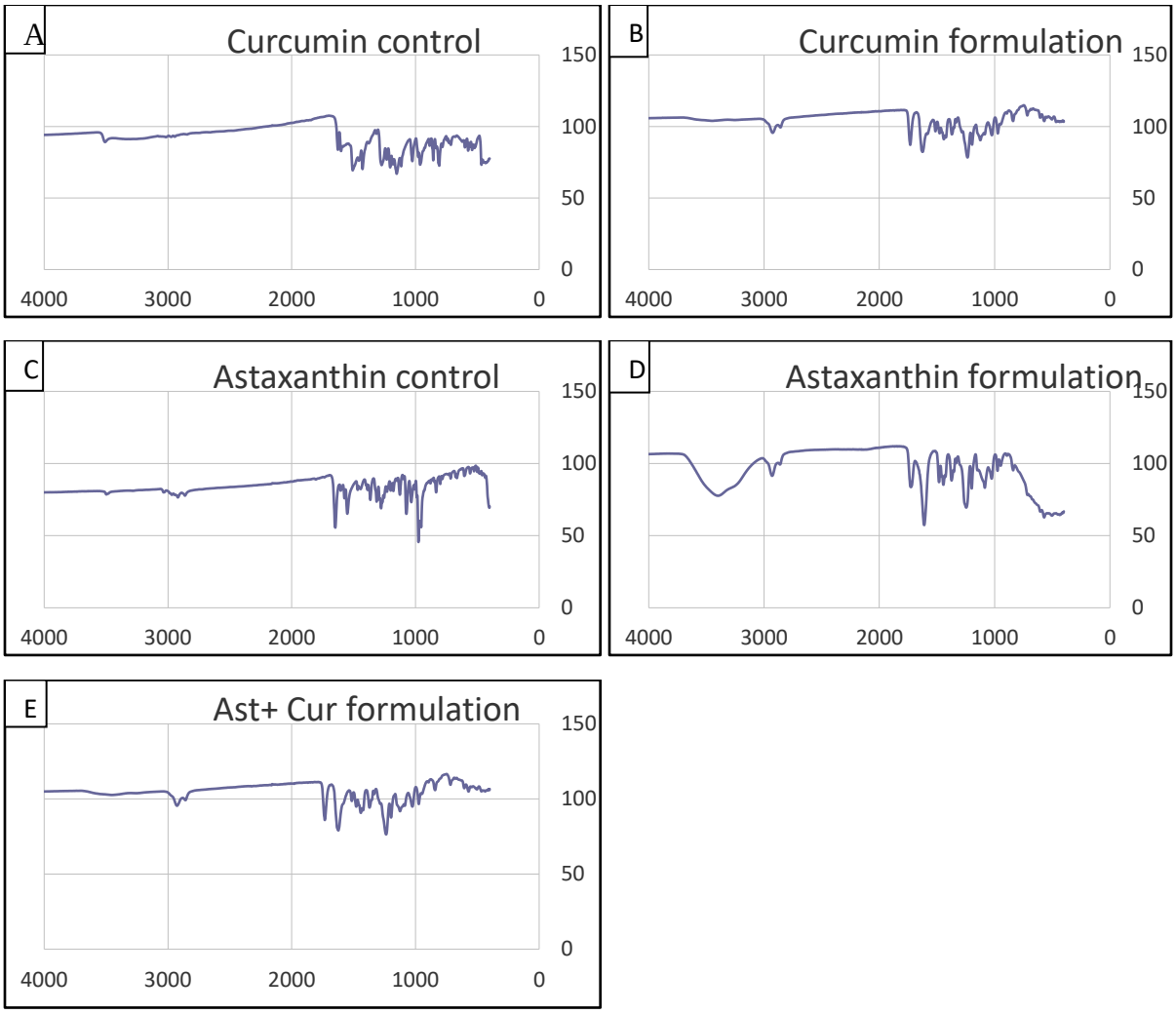

Figure 4.1 The IR Spectra images of A- CUR (control), B- CUR SD, C- AST (control), D- AST SD, E- SD of the combination of AST & CUR.

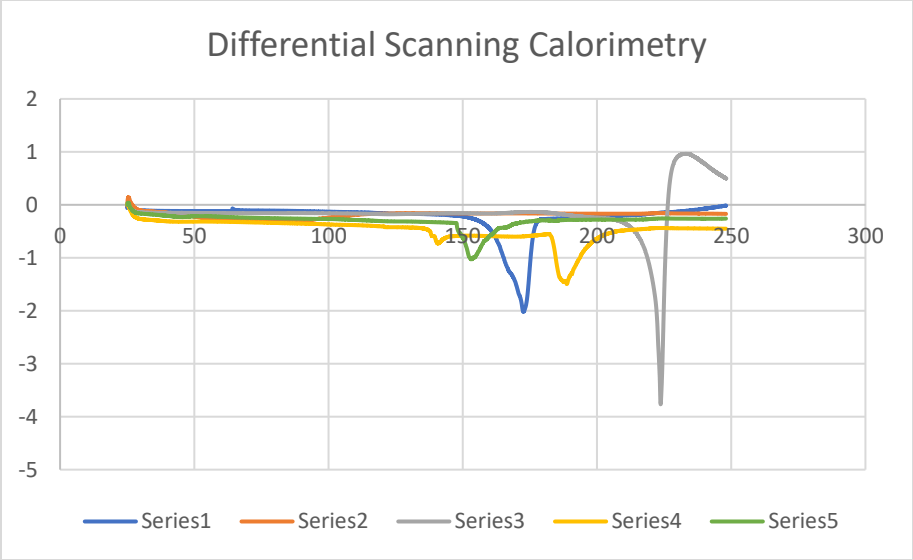

Figure 4.2The DSC analysis of SD of AST, CUR, & AT CUR combination where Series 1- Free CUR, Series 2- SD of CUR, 3- Free AST, 4- SD of AST, 5- SD of AST+ CUR.

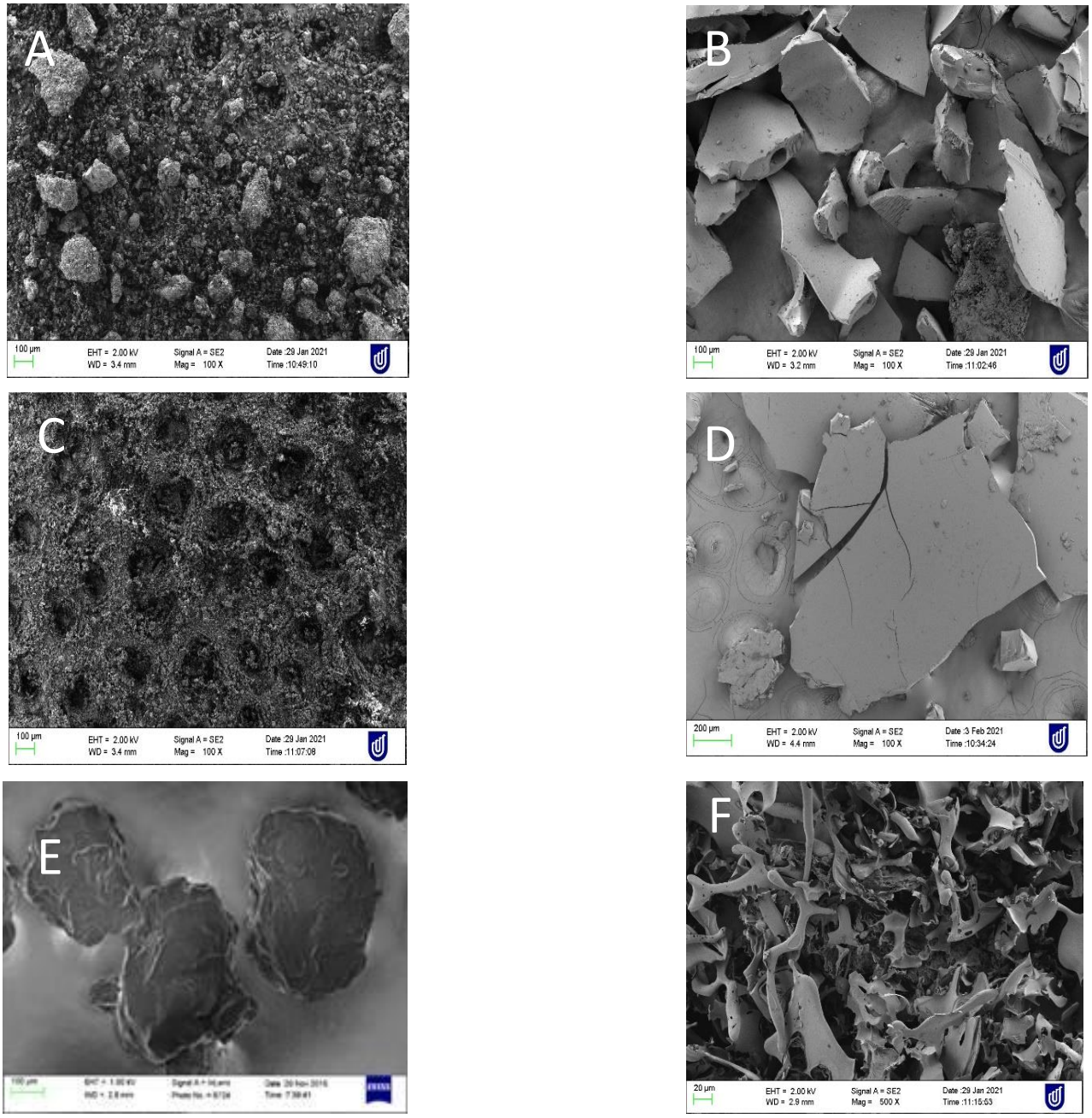

Figure 4.3 A- Free CUR particles, B- CUR and SOL formulation, C- Free AST particles, D- AST and SOL formulation, E- SOL as observed under SEM, F- Combination of AST and CUR micelle formed using SOL.

4.4 Cytotoxic assay

MTT assay was carried out with free AST, CUR, and combination of AST and CUR to determine IC 50 value. The IC50 value of AST was 7.77 µg/ml (Figure 4.4), CUR was 10.44 µg/ml (Figure 4.5), and the combination of AST and CUR was 8.91 µg/ml (Figure 4.6). The IC50 value of 5-FU was 13.89 µg/ml. The standard error of the mean and standard deviation was for an experiment carried in triplicate where (n=3).

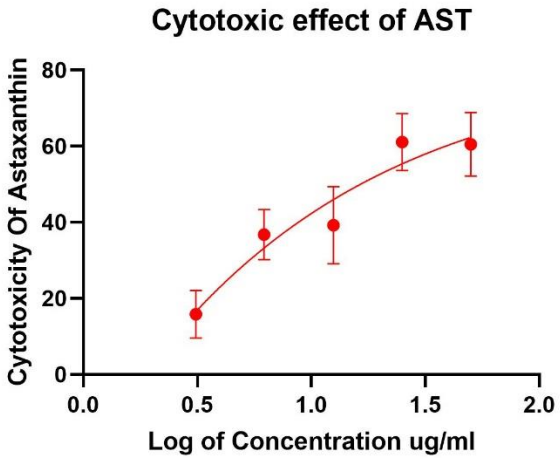

Figure 4.4 IC50 value of AST.

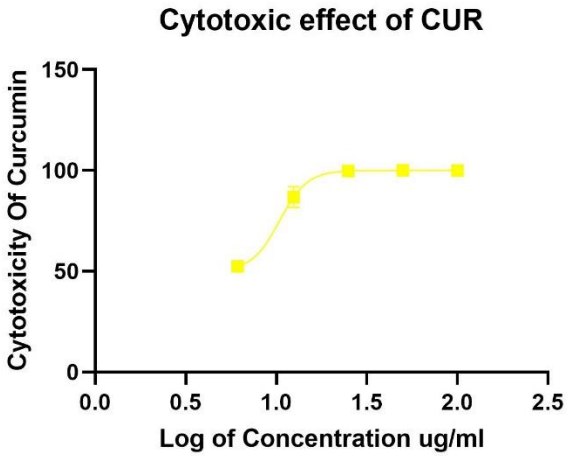

Figure 4.5 IC50 value of CUR.

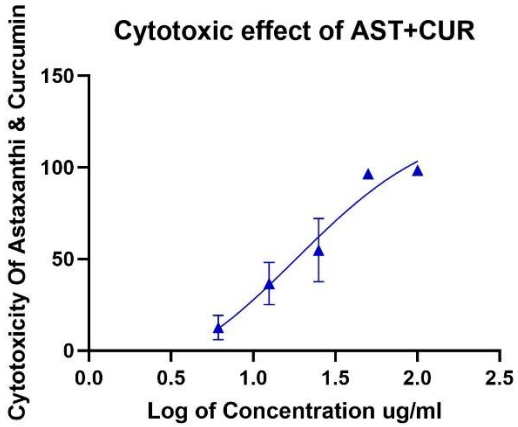

Figure 4.6 IC50 value of AST And CUR.

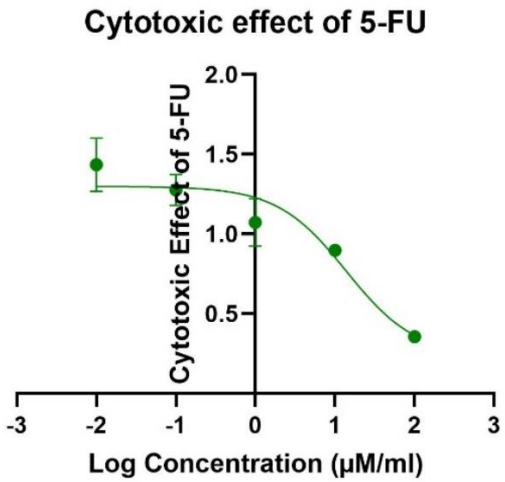

Figure 4.7 Cytotoxic effect of 5-FU

When HCT-116 cells were treated with free AST dissolved in water and DMSO, it showed significant cytotoxicity when dissolved in DMSO as compared to water. After 48 h 48.6% and 54.3% cytotoxicity were observed when dissolved in water and DMSO respectively at the highest concentration. It was evident that micellized AST, when dissolved in water and DMSO, showcased consistent dose-dependent cytotoxic effect as opposed to free AST which only gave dose-response

when dissolved in DMSO. Its cytotoxicity was 85% and 51.4% when dissolved in water and DMSO respectively. The p-value of SD of AST v/s AST dissolved in water is <0.0001 (****).

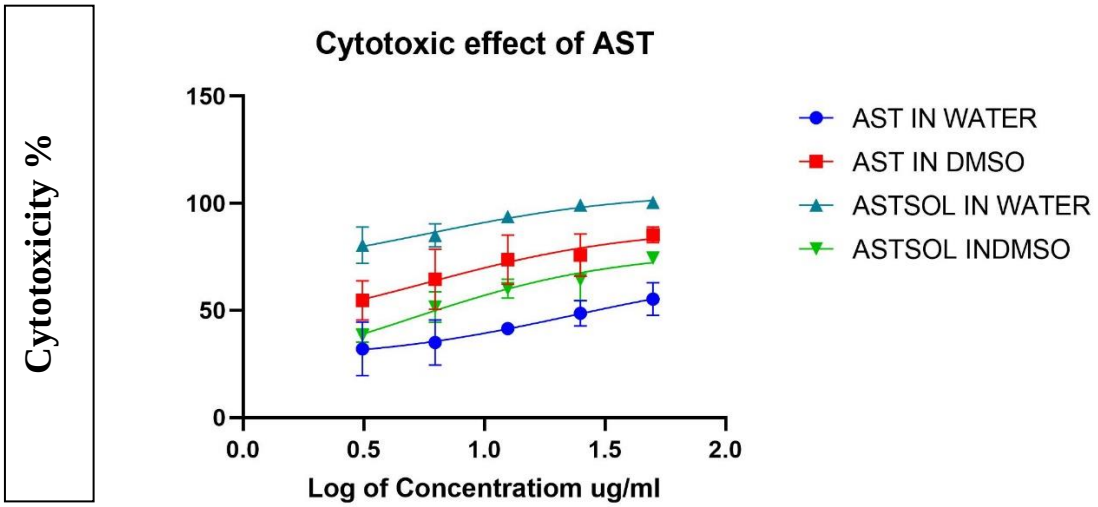

Figure 4.8 IC 50 values of AST dissolved in water (Blue) and DMSO (Red), SD of AST dissolved in water (Teal) and DMSO (Green). (p-value of SD of AST v/s AST dissolved in water is <0.0001 (****), and p values of AST and SD of AST dissolved in DMSO is 0.1421).

When CUR showed a significant cytotoxic effect of 86.8% when dissolved in DMSO as compared to water which only showed a 77.7% cytotoxic effect after 48 h treatment. Similarly, when micellized CUR was dissolved in DMSO it also exhibited a dose-dependent cytotoxic effect in contrast with free CUR dissolved in water. It was observed that its cytotoxic effect was of 85.1% and 92.2% when dissolved in water and DMSO respectively. But, p-value of SD of CUR v/s CUR dissolved in water is 0.3017. The p values of AST and SD of AST, as well as CUR and SD of CUR dissolved in DMSO are p= 0.1421 and p= 0.2881, respectively.

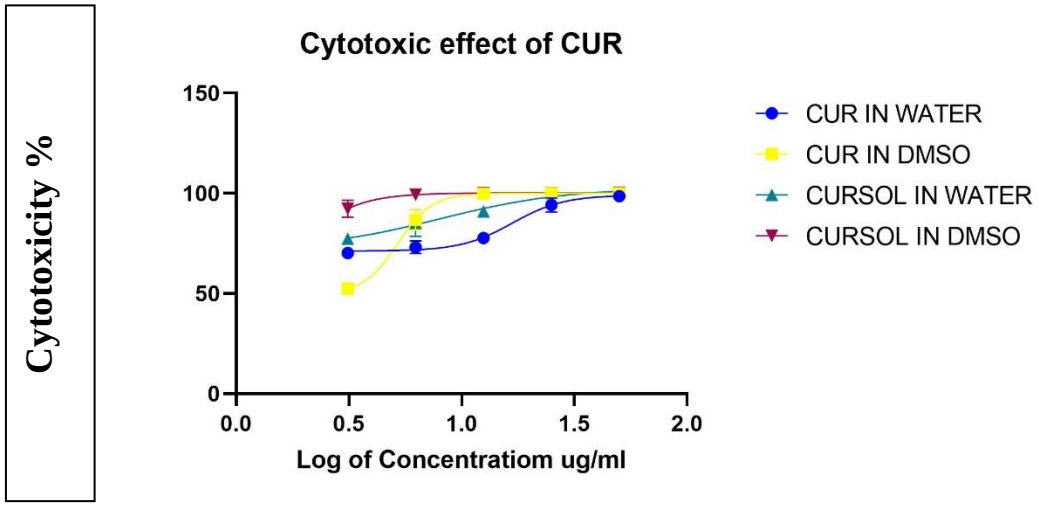

Figure 4.9 IC50 values of CUR dissolved in water (Blue) and DMSO (Yellow), and SD of CUR dissolved in water (Teal) and DMSO (Magenta). (p-value of SD of CUR v/s CUR dissolved in water is 0.3017, and CUR and SD of CUR dissolved in DMSO is 0.2881).

When the combination of AST and CUR was used a similar trend of higher cytotoxic effect of 98.4 % with DMSO was observed as opposed to cytotoxic effect in water of 79.9%. In all the treatments when the drug or the combination of the drug was dissolved in water inconsistencies were observed in cytotoxic activity in replicates. This could be due to the drug being insoluble in water and not being equally distributed in the wells when treated.

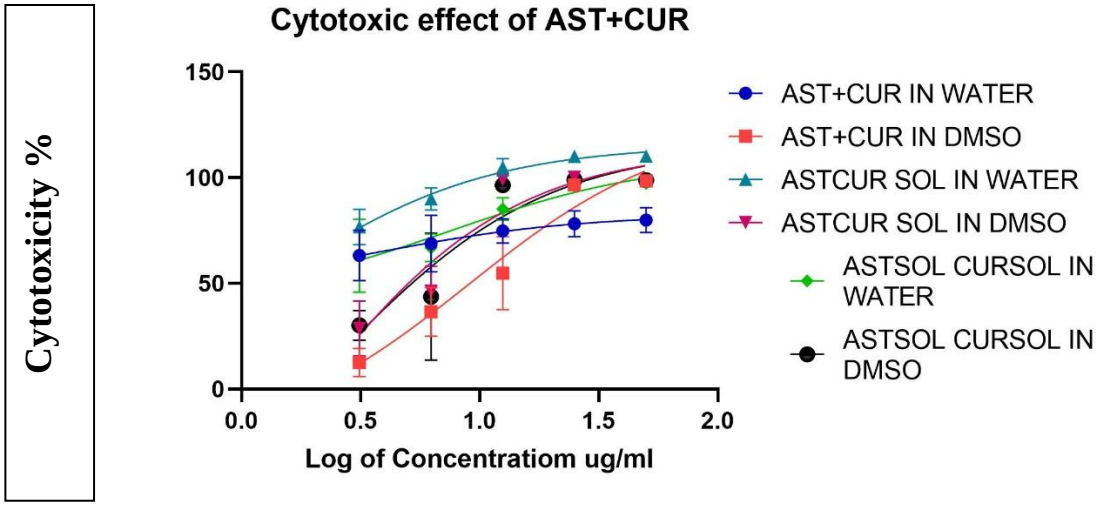

Figure 4.10 IC50 value of combination of AST and CUR dissolved in water (Blue) and DMSO (Red), SD of AST and CUR dissolved in water (Teal) and DMSO (Magenta), and SD of AST and SD of CUR dissolved in water (Green) and DMSO (Black) simultaneously. (p-value of SD of combination of AST and CUR against combination of free AST and CUR dissolved in water is 0.0081 (**) and SD of AST and CUR against AST and CUR, dissolved in DMSO is 0.5367)

HCT-116 cells were treated in two different ways with a combination of micellized AST CUR. The cytotoxic effect of micellized AST and CUR administered individually at equal concentration dissolved in water and DMSO were 97.2% and 98.8%. Whereas the cytotoxic effect of the combination of micellized AST and CUR was 89.9% in water and 98.1% in DMSO. The p-value of SD of combination of AST and CUR against combination of free AST and CUR dissolved in water is 0.0081 (**). Whereas the p-value of SD of AST and CUR administered individually to form combination against combination of free AST and CUR dissolved in water was 0.2994. The p-value SD of combination of AST and CUR against SD of AST and CUR administered individually is 0.1259. The p values of SD of AST and CUR against AST and CUR, SD of AST and CUR administered individually against AST and CUR, and SD of AST and CUR against SD

of AST and CUR administered individually dissolved in DMSO is 0.5367, 0.55670, and 0.1259 respectively.

Chapter 5 Discussions

5.1 Solubility

The aqueous solubility increased approximately 145- fold for SD of AST and 9700- folds for SD of CUR, whereas the SD of the combination of AST and CUR had 114- 237- fold increment in the aqueous solubility. In a study where SOL was used to form SD of CUR, the solubility improvement was 5800- fold. The aqueous solubility of AST has not been reported yet, and it is poorly soluble in organic solvents with only 0.025 to 3.7 µg/ml AST being soluble in dichloromethane. When Captisol was used to improve the aqueous solubility of AST, it resulted in 71- fold improvement in solubility, whereas the solubility improvement in this study was approximately 2 times more. Captisol is a sulfobutyl ether β-cyclodextrin used to improve solubility, bioavailability, and stability of a compound (Lockwood et al., 2003). The solubility improvement in this study was 1.67 times more as compared to the previous study (Parikh et al., 2018). This drastic improvement in solubility is suggestive of the transformation of AST and CUR from crystalline to amorphous form which improves the bioavailability of the compounds.

5.2 Entrapment efficiency and loading ability

As expected, the SD with the highest concentration of polymer SOL had the highest solubility. It also had the highest entrapment efficiency as well as loading ability for SD of CUR, SD of AST, and SD of AST and CUR combination. Thus, it can be concluded that CUR and AST successfully formed self-nanomicellizing SDs. In the case of CUR entrapment efficiency and loading ability is 95.6% and 10.6% which more than 87% and 7% respectively as observed in another study (Liu et al., 2016a). For AST, encapsulation efficiency (15.31%) and loading ability (1.7%) was

comparatively less than previous literature where encapsulation efficiency was 93.5% (Liu et al., 2019a). This could be due to the low quantity of AST available for the preparation of SD. It could also be due to the procedure used to prepare SD which resulted in a loss of AST.

5.3 Characterization

5.3.1 FTIR

CUR showed characteristic -OH phenolic stretching vibrations at 3512 cm^{-1}, benzene ring stretching vibrations at 1602 cm^{-1}, carbonyl (C=C), enol (C–O) stretching vibrations at 1507 cm^{-1}, olefinic -C-H bending vibrations at 1428 cm^{-1}, aromatic -C-O vibrations at 1274 cm^{-1}, and -C-O-C methoxy vibrations at 1153 cm^{-1}. SOL showed 1735 cm^{-1}, 2860 cm^{-1}, and 3469 cm^{-1} for carbonyl, aliphatic C–H stretching, and hydroxyl groups. The SD of CUR showed peak broadening from 3374 to 3637 cm^{-1} which is characteristic for CUR and SOL, but no peak shifting of vibrations at 1274 cm^{-1}, 1428 cm^{-1}, 1507 cm^{-1}, and 1602 cm^{-1} of CUR or at 1735 cm^{-1}, and 2860 cm^{-1} of SOL (Yallapu et al., 2010) (Parikh et al., 2018). The peak broadening at phenolic region suggests an interaction between the drug and polymer via hydrogen bond is due to carbonyl and hydroxyl group's involvement. In case of AST control there was a sharp characteristic peak at 1649 cm^{-1} which is C=O stretching vibration, 1549 cm^{-1} for C=C stretching vibration in the aromatic ring, and 975 cm^{-1} which is for C=H (Yuan et al., 2012). The characteristic curve of AST and SOL were not shifting, although there was broadening of the peak from 3269 to 3647 cm^{-1} which is characteristic vibration for AST and SOL was observed indicating carbonyl and hydroxyl involvement in hydrogen bonding of drug and polymer. The SD of the combination of AST and CUR involved all characteristic signals of AST, CUR, and SOL and similar carbonyl and hydroxyl

involvement in hydrogen bond formation with the polymer suggestive from peak broadening around 3340 to 3587 cm $^{-1}$.

5.3.2 Differential scanning calorimetry

The endothermic peak of CUR was 172.54°C close to 183°C which is reported as the melting point of CUR but for SD of CUR, it was reduced to approximately 81.16. Similarly, the melting point of AST is 223.67 °C close to 216°C which is reported as the melting point of AST, but SD of AST has its Tm reduced to 187.29 °C. Meanwhile, SD of the combination of AST and CUR is 152.99 °C which is lower than the melting point of both the compounds. This endothermic shift indicates a strong drug to carrier interaction. Thus, confirming that drug has been micellized within the polymer. Changes in the thermal event also indicate the conversion of a drug from solid crystalline state to amorphous state (Yallapu et al., 2010, Parikh et al., 2018). In one of these studies, the Tm achieved was 167 °C, while in the current study the Tm is 81.16 °C which is lower than that suggesting stronger bonding between SOL and CUR (Parikh et al., 2018). In a recent study, the endothermic peak of nano-dispersed AST was nearly 100 °C. They also concluded AST to be in amorphous form (Shen et al., 2018). The shifting of the peak also confirms the solid-state change in the SD.

5.3.3 SEM

Free AST is densely clumped, but SD of AST appears in amorphous form. Free CUR was observed as aggregates and no uniform size distribution which results in an unequal distribution of a drug. Free CUR is in crystalline form based on its morphology. SD of CUR is uniformly distributed and in amorphous form as no crystalline CUR like morphology was found. The purpose of making SD of AST and CUR combined as a more bioavailable drug was achieved by it being uniformly

distributed in an amorphous state as it appears like a thin film structure with the help of SOL. It can be said that there is uniform size distribution as no aggregates of different sizes are observed. All the SD form glass-like film structures which is a typical characteristic when using polymer. SEM results indicate that SOL helps both AST and CUR and its combination exist in an amorphous state which improves the solubility of the drug (Fule and Amin, 2014). SEM results also proved uniform distribution of both the drugs in the formulation and strong interactions which is consistent with the results of DSC.

5.4 Cytotoxic assay

The IC50 value of AST (7.7 µg/ml) (Liu et al., 2016b) and CUR (10.4 µg/ml) (Bolat et al., 2020) after 48 h of treatment was close to what was found in the literature. The IC50 value of free AST when dissolved in water is 23.13 µg/ml and DMSO is 5.76 µg/ml respectively. The IC50 value of free CUR dissolved in water is 16.78 µg/ml and in DMSO is 5.21 µg/ml respectively. The IC50 values of the combination of free AST and CUR dissolved in water and DMSO were 3.62 µg/ml and 8.97 µg/ml respectively.

The IC50 value of micellized AST dissolved in water is 5.71 µg/ml and in DMSO is 4.82 µg/ml which is less than free AST. It proves that micellized AST has enhanced cytotoxic effect on HCT-116 cells as compared to free AST. The IC50 values of SD of CUR were 7.98 µg/ml and 1.66 µg/ml when dissolved in water and DMSO respectively which suggests that micellized CUR has amplified cytotoxic effect against HCT-116 colon cancer cells.

The IC50 value of combination dose administered by adding SD of AST and SD of CUR individually at equal concentration dissolved in water and DMSO are 7.65 µg/ml and 2.61 µg/ml,

respectively. While the IC50 value of the combination of SD of AST and CUR dissolved in water and DMSO were 1.46 µg/ml and 1.83 µg/ml.

The IC50 values of micellized AST and CUR were low as compared to free AST and CUR suggesting that the micellized formulation has augmented cytotoxic effect on HCT-116 cells. The cytotoxic effect significant as p-value of SD of AST v/s AST is ($p<0.05$), but p-value of SD of CUR v/s CUR dissolved in water is non significant ($p>0.05$). The p values of AST and SD of AST, as well as CUR and SD of CUR dissolved in DMSO does not display any significance ($p>0.05$).

In comparison, the combination of SD of AST and CUR also has significant increase cytotoxicity as its IC50 value is lower than the combination of free AST and CUR. The p-value of SD of combination of AST and CUR against combination of free AST and CUR dissolved in water is significant ($p<0.05$), Whereas the p-value of SD of AST and CUR administered individually to form combination against combination of free AST and CUR dissolved in water was not significant ($p>0.05$). The p-value SD of combination of AST and CUR against SD of AST and CUR administered individually dissolved in water is also not significant ($p>0.05$). The p-value SD of combination of AST and CUR against SD of AST and CUR administered individually is 0.1259. The p values of SD of AST and CUR against AST and CUR, SD of AST and CUR administered individually against AST and CUR, and SD of AST and CUR against SD of AST and CUR administered individually dissolved in DMSO is non significant ($p>0.005$).

All this data suggests that SD of AST, SD of CUR, and SD of AST and CUR combination dissolved in water has significantly higher cytotoxicity as compared to free AST, CUR, and combination of AST and CUR dissolved in water. Thus, it is evident that SDs have increased the solubility and bioavailability of the compounds and increased its cytotoxic effect. When dissolved

in DMSO no significant increase in cytotoxicity is observed as the compounds were soluble in DMSO prior to micellization as well.

Solubility test, SEM, DSC, FTIR, as well as cytotoxic activity results suggest that bioavailability of AST and CUR has increased. In this study, AST and CUR are dissolved in both water and DMSO. Both the compounds which are in their natural form insoluble or poorly soluble in water are soluble in water when SOL is used to form self- nanomicellizing SD. Thus, the amorphous self-nanomicellizing structure has increased solubility and in turn, increased bioavailability of the drug to be more effective.

As mentioned in the literature review, AST and CUR have been used against cancer cell lines when dissolved in DMSO which is a hazardous organic solvent and itself is cytotoxic to cancer cells. The formation of SD can be used to investigate the drug's cytotoxic effect more accurately without any interference from DMSO.

Stereoisomers of AST were used against HCT-116 cells in a study and the apoptotic cells of approximately 30% were found when treated with the isomers (Liu et al., 2016b). In this study, SD of AST dissolved in water itself had the cytotoxic activity of 85% and 51.4% when dissolved in DMSO. There is a significant increase in the cytotoxic activity of the compound compared to the literature as the solubility of the compound has significantly increased.

In comparison, the cytotoxic effect of approximately 98% against HT-29 and AGS cells was observed when nanoemulsion of AST was formed (Shanmugpriya et al, 2018). This is consistent with the current study. Although in the previous study, nanoemulsions were formed and in this study nanomicelles were formed, the data is suggestive that bioavailability of the compound is

increased which results in increased cytotoxic effect. Thus, it can be considered that the SD of AST has higher cytotoxicity as compared to free AST.

Emulsomes were used in a study and cell viability of 50% was reported (Bolat et al., 2020). In contrast, the cytotoxic activity of 85.1% and 92.2% were found in this study when SD of CUR was dissolved in water and DMSO respectively. Free CUR showed around 43% cell proliferation and encapsulated CUR showed approximately 50% cell inhibition after 48 h of treatment (Jayaprakasha et al., 2016). However, cytotoxic effect in this study is significantly higher. This is consistent with the literature review where nanomicelles are stated as the best approach to increase the bioavailability of a compound and make it more effective as a drug.

A combination of AST and CUR has not been used as an anti-cancer drug. In this study, a SD of the combination of AST and CUR is successfully prepared. It has similar characteristics to the compound's individual SD. It also has increased solubility and bioavailability. The cytotoxic effect is 89.9% and 98.1% when dissolved in water and DMSO which is significantly more than the SD of AST and SD of CUR.

5.5 Limitation

AST is an expensive bioactive compound and available in very low quantities in the market. Due to the covid- 19 pandemic only low quantities of AST was procured. As a result, the same method of preparation of SD which was applied to CUR could not be applied to AST. An entirely different approach had to be taken for preparing SDs for AST which was highly time and energy consuming approach. It required more than 48 h for freeze-drying the AST-SOL mixture to obtain it in solid form.

Two different methods of HPLC analysis were employed for 2 different compounds. This resulted in drastic variations in solubility, entrapment efficiency and loading ability results obtained from both the HPLC equipment for the SD containing a combination of AST and CUR. Since the purpose was to develop a SD containing both AST and CUR, HPLC method which can detect the presence of both the compound is required. The column used for both the methods was same and CUR has a retention time of 2.7 whereas AST has a retention time of 2.9.

It was challenging to work with both the compounds as they are poorly soluble. Sonication had to be done to obtain a clear solution. It was challenging to use it as a treatment for HCT-116 cells and carry out cytotoxic assay as the compounds themselves are highly coloured and interfere with the reading of optical density. Hence, it was time-consuming to obtain the IC50 values of the compounds. Only 66% purity of CUR prevents determination of accurate cytotoxic activity by the compound.

Due to time constraints during this pandemic, the cytotoxic assay was carried out as soon as SD was prepared based on the IC50 values of the crude compound without data of entrapment efficiency or loading ability. Hence, the actual concentration resulting in significant cytotoxic effect may be lower than what was calculated. So, the SD of combination is more effective in promoting apoptosis in HCT-116 cells and has a lower IC50 value which should be investigated once more compound is available.

5.6 Future prospective

The future prospect for this study is to meet all the limitations. Development of a common HPLC method for both the compounds. Both the compounds have a retention time close to 2.8 and are compatible with the same column.

Characterization of the SDs has been done. Stability tests of the SD should be carried out which include but are not limited to stability in varied pH, temperature, and oxidative stress.

In- vitro testing with a different drug to drug (AST to CUR) ratio in the SD should be carried out. *In- vitro* testing should be carried out considering the entrapment efficiency and loading ability of the compounds to administer the correct dosage. *In- vitro* testing with different cell lines should be done. Cytotoxicity against healthy cells should be investigated and stage of apoptosis should be determined. If all *in- vitro* tests are successful, *in- vivo* testing should also be considered. All significant findings should be published.

Chapter 6 Conclusion

In conclusion, SD of AST, CUR, and combination of AST and CUR was successfully achieved using SOL as the polymer. The compound which was initially present in crystalline structure has been transformed into the uniformly distributed amorphous structure. This self-nanomicellizing SD of AST and CUR had solubility of 3.67 µg/ml and 5285.5 µg/ml and the SD of a combination of AST and CUR had CUR with the solubility of 128.03 µg/ml and AST with the solubility of 2.85 µg/ml. This accounts for approximately 145, 9700, 237, and 114- fold increase in solubility each, respectively.

The entrapment efficiency of SD of AST (1:9), SD of CUR (1:9), AST in SD of AST and CUR, and CUR in SD of AST and CUR (1:9) is 15.31%, 95.6%, 92.55%, and 12.67% respectively, whereas the loading ability of SD of AST (1:9), SD of CUR (1:9), AST in SD of AST and CUR, and CUR in SD of AST and CUR (1:9) is1.7%, 10.62%, 10.28%, and 1.4% respectively

The bioavailability of the previously poorly soluble compound has increased. The cytotoxic effect of SD of AST is 85% when dissolved in water and 51.4% when dissolved in DMSO, whereas it is 85.1% and 92.2% when SD of CUR was dissolved in water and DMSO respectively. As hypothesized SD of a combination of AST and CUR has synergistic cytotoxic effect of 89.9% and 98.1% when dissolved in water and DMSO. The cytotoxicity of the drug increased in a dose-dependent manner. The IC50 values for the combination of SD of AST and CUR is also very low (1.46 µg/ml and 1.83 µg/ml) which suggests that it can be used as a potential complimentary treatment for cancer without administering harmful high doses.

Chapter 7 References

[Figure 1.1 Estimate of most common cancers diagnosed in 2020
<https://www.canceraustralia.gov.au/affected-cancer/cancer-types/bowel-cancer/bowel-cancer-colorectal-cancer-australia-statistics>
Figure 2.1 Astaxanthin structure, Pubchem

<https://pubchem.ncbi.nlm.nih.gov/compound/Astaxanthin#section=2D-Structure>

Figure 2.2 Metabolic effects of astaxanthin causing apoptosis
Kavitha, K., Kowshik, J., Kishore, T. K. K., Baba, A. B. & Nagini, S. 2013, "Astaxanthin inhibits NF-κB and Wnt/β-catenin signalling pathways via inactivation of Erk/MAPK and PI3K/Akt to induce intrinsic apoptosis in a hamster model of oral cancer", *Biochimica et Biophysica Acta -General Subjects,* 1830**,** 4433-4444.
Figure 2.3 Curcumin structure,

Farazuddin, M., Dua, B., Zia, Q., Khan, A. A., Joshi, B. & Owais, M. 2014, "Chemotherapeutic potential of curcumin-bearing microcells against hepatocellular carcinoma in model animals", *International Journal of Nanomedicine,* 9**,** 1139.
Figure 2.4 Effect of CUR on tp53 and apoptosis pathways resulting in cell death
Mccubrey, J. A., Lertpiriyapong, K., Steelman, L. S., Abrams, S. L., Yang, L. V., Murata, R. M., Rosalen, P. L., Scalisi, A., Neri, L. M. & Cocco, L. 2017, "Effects of resveratrol, curcumin, berberine and other nutraceuticals on aging, cancer development, cancer stem cells and microRNAs", *Aging,* 9**,** 1477.
Figure 2.5 Soluplus structure,

Noh, G., Keum, T., Seo, J.-E., Choi, J., Rakesh, B., Shrawani, L., Park, B., Choi, Y. W. & Lee, S. 2018, "Development and evaluation of a water soluble fluorometholone eye drop formulation employing polymeric micelle", *Pharmaceutics,* 10**,** 208.

Figure 2.6 Drug entrapped within polymer resulting in SD formation
Vaka, S. R. K., Bommana, M. M., Desai, D., Djordjevic, J., Phuapradit, W. & Shah, N. 2014, "Excipients for amorphous solid dispersions", excerpt from *Amorphous Solid Dispersions,* Springer, 123-161.]

[AST price Sigma Aldrich., 2020
<https://www.sigmaaldrich.com/catalog/product/sigma/sml0982?lang=en&region=AU>

Astaxanthin Market Analysis Report, 2020

<https://www.grandviewresearch.com/industry-analysis/global-astaxanthin-market#:~:text=Natural%20astaxanthin%20dominated%20the%20overall,supplements%2C%20and%20low%20maintenance%20costs.>

Cancer Australia, 2020
<https://www.canceraustralia.gov.au/affected-cancer/cancer-types/bowel-cancer/bowel-cancer-colorectal-cancer-australia-statistics>
CUR price Sigma Aldrich, 2020
<https://www.sigmaaldrich.com/catalog/product/sigma/c1386?lang=en&region=AU&cm_sp=Insite-_-caSrpResults_srpRecs_srpModel_curcumin-_-srpRecs3-1>

Curcumin Market Analysis Report, 2020

<https://www.grandviewresearch.com/industry-analysis/turmeric-extract-curcumin-market#:~:text=The%20global%20curcumin%20market%20size,use%20across%20end%2Duser%20industries>
Market Data Forecast, 2020
<https://www.marketdataforecast.com/market-reports/polymer-dispersions-market>]

Abandansari, H. S., Abuali, M., Nabid, M. R. & Niknejad, H. 2017, "Enhance chemotherapy efficacy and minimize anticancer drug side effects by using reversibly pH-and redox-responsive cross-linked unimolecular micelles", *Polymer,* 116**,** 16-26.

Affandi, M. M. M., Julianto, T. & Majeed, A. 2012, "Enhanced oral bioavailability of astaxanthin with droplet size reduction", *Food Science and Technology Research,* 18**,** 549-554.

Ajji, P. K., Walder, K. & Puri, M. 2020, "Combination of Balsamin and flavonoids induce apoptotic effects in liver and breast cancer cells", *Frontiers in Pharmacology,* 11.

Ambati, R. R., Phang, S.-M., Ravi, S. & Aswathanarayana, R. G. 2014, "Astaxanthin: sources, extraction, stability, biological activities and its commercial applications—a review", *Marine Drugs,* 12**,** 128-152.

Batra, H., Pawar, S. & Bahl, D. 2019, "Curcumin in combination with anti-cancer drugs: A nanomedicine review", *Pharmacological Research,* 139**,** 91-105.

Bergonzi, M., Hamdouch, R., Mazzacuva, F., Isacchi, B. & Bilia, A. 2014, "Optimization, characterization and in vitro evaluation of curcumin microemulsions", *LWT-Food Science and Technology,* 59**,** 148-155.

Bernabeu, E., Gonzalez, L., Cagel, M., Gergic, E. P., Moretton, M. A. & Chiappetta, D. A. 2016, "Novel Soluplus®—TPGS mixed micelles for encapsulation of paclitaxel with enhanced in vitro cytotoxicity on breast and ovarian cancer cell lines", *Colloids Surfaces B: Biointerfaces,* 140**,** 403-411.

Bharathiraja, S., Manivasagan, P., Quang Bui, N., Oh, Y.-O., Lim, I. G., Park, S. & Oh, J. 2016, "Cytotoxic induction and photoacoustic imaging of breast cancer cells using astaxanthin-reduced gold nanoparticles", *Nanomaterials,* 6**,** 78.

Birudaraju, D., Cherukuri, L., Kinninger, A., Chaganti, B. T., Shaikh, K., Hamal, S., Flores, F., Roy, S. K. & Budoff, M. J. 2020, "A combined effect of Cavacurcumin, Eicosapentaenoic acid (Omega-3s), Astaxanthin and Gamma–linoleic acid (Omega-6)(CEAG) in healthy volunteers-a randomized, double-blind, placebo-controlled study", *Clinical Nutrition ESPEN,* 35**,** 174-179.

Bolat, Z. B., Islek, Z., Demir, B. N., Yilmaz, E. N., Sahin, F. & Ucisik, M. H. 2020, "Curcumin-and Piperine-loaded emulsomes as combinational treatment approach enhance the anticancer activity of Curcumin on HCT116 colorectal cancer model", *Frontiers in Bioengineering Biotechnology,* 8**,** 50.

Bush, P. A. & Noe, J. F. 2020, "Immunotherapy and Targeted Drugs for Common Cancers", *The Journal for Nurse Practitioners,* 16**,** 195-200.

Carvalho, C., Santos, R. X., Cardoso, S., Correia, S., Oliveira, P. J., Santos, M. S. & Moreira, P. I. 2009, "Doxorubicin: the good, the bad and the ugly effect", *Current Medicinal Chemistry,* 16**,** 3267-3285.

Chen, Y.-T., Kao, C.-J., Huang, H.-Y., Huang, S.-Y., Chen, C.-Y., Lin, Y.-S., Wen, Z.-H. & Wang, H.-M. D. 2017, "Astaxanthin reduces MMP expressions, suppresses cancer cell migrations, and triggers apoptotic caspases of in vitro and in vivo models in melanoma", *Journal of Functional Foods,* 31**,** 20-31.

Cottart, C. H., Nivet-Antoine, V. & Beaudeux, J. L. 2014, "Review of recent data on the metabolism, biological effects, and toxicity of resveratrol in humans", *Molecular Nutrition & Food Research,* 58**,** 7-21.

Cottart, C. H., Nivet-Antoine, V., Laguillier-Morizot, C. & Beaudeux, J. L. 2010, "Resveratrol bioavailability and toxicity in humans", *Molecular Nutrition & Food Research,* 54**,** 7-16.

De Matos, R. P. A., Calmon, M. F., Amantino, C. F., Villa, L. L., Primo, F. L., Tedesco, A. C. & Rahal, P. 2018, "Effect of curcumin-nanoemulsion associated with photodynamic therapy in cervical carcinoma cell lines", *BioMed Research International,* 2018.

Dian, L., Yu, E., Chen, X., Wen, X., Zhang, Z., Qin, L., Wang, Q., Li, G. & Wu, C. 2014, "Enhancing oral bioavailability of quercetin using novel soluplus polymeric micelles", *Nanoscale Research Letters,* 9**,** 684.

Doktorovova, S., Souto, E. B. & Silva, A. M. 2018, "Hansen solubility parameters (HSP) for prescreening formulation of solid lipid nanoparticles (SLN): in vitro testing of curcumin-loaded SLN in MCF-7 and BT-474 cell lines", *Pharmaceutical Development Technology,* 23**,** 96-105.

Edelman, R., Engelberg, S., Fahoum, L., Meyron-Holtz, E. G. & Livney, Y. D. 2019, "Potato protein-based carriers for enhancing bioavailability of astaxanthin", *Food Hydrocolloids,* 96**,** 72-80.

Eder, A. R. & Arriaga, E. A. 2006, "Capillary electrophoresis monitors enhancement in subcellular reactive oxygen species production upon treatment with doxorubicin", *Chemical Research in Toxicology,* 19**,** 1151-1159.

Faraone, I., Sinisgalli, C., Ostuni, A., Armentano, M. F., Carmosino, M., Milella, L., Russo, D., Labanca, F. & Khan, H. 2020, "Astaxanthin anticancer effects are mediated through multiple molecular mechanisms: a systematic review", *Pharmacological Research***,** 104689.

Ferlay, J., Colombet, M., Soerjomataram, I., Mathers, C., Parkin, D., Piñeros, M., Znaor, A. & Bray, F. 2019, "Estimating the global cancer incidence and mortality in 2018: GLOBOCAN sources and methods", *International Journal of Cancer,* 144**,** 1941-1953.

Fule, R. & Amin, P. 2014, "Development and evaluation of lafutidine solid dispersion via hot-melt extrusion: investigating drug-polymer miscibility with advanced characterisation", *Asian Journal of Pharmaceutical Sciences,* 9**,** 92-106.

Gao, A., Hu, X.-L., Saeed, M., Chen, B.-F., Li, Y.-P. & Yu, H.-J. 2019, "Overview of recent advances in liposomal nanoparticle-based cancer immunotherapy", *Acta Pharmacological Sinica,* 40**,** 1129-1137.

Gera, M., Sharma, N., Ghosh, M., Huynh, D. L., Lee, S. J., Min, T., Kwon, T. & Jeong, D. K. 2017, "Nanoformulations of curcumin: an emerging paradigm for improved remedial application", *Oncotarget,* 8**,** 66680.

Hortobagyi, G. 1997, "Anthracyclines in the treatment of cancer", *Drugs,* 54**,** 1-7.

Homayouni, A., Amini, M., Sohrabi, M., Varshosaz, J. & Nokhodchi, A. 2019, "Curcumin nanoparticles containing poloxamer or soluplus tailored by high-pressure homogenization using antisolvent crystallization", *International Journal of Pharmaceutics,* 562**,** 124-134.

Jayaprakasha, G. K., Murthy, K. N. C. & Patil, B. S. 2016, "Enhanced colon cancer chemoprevention of curcumin by nanoencapsulation with whey protein", *European Journal of Pharmacology,* 789**,** 291-300.

Kamal, M. M., Salawi, A., Lam, M., Nokhodchi, A., Abu-Fayyad, A., El Sayed, K. A. & Nazzal, S. 2020, "Development and characterization of curcumin-loaded solid self-emulsifying drug delivery system (SEDDS) by spray drying using Soluplus® as solid carrier", *Powder Technology,* 369**,** 137-145.

Karanam, G., Arumugam, M. K. & Natesh, N. S. 2020, "Anticancer effect of marine sponge-associated *Bacillus pumilus* amk1 derived dipeptide cyclo (-pro-tyr) in human liver cancer cell line through apoptosis and G2/M phase arrest", *International Journal of Peptide Research Therapeutics,* 26**,** 445-457.

Kavitha, K., Kowshik, J., Kishore, T. K. K., Baba, A. B. & Nagini, S. 2013, "Astaxanthin inhibits NF-κB and Wnt/β-catenin signalling pathways via inactivation of Erk/MAPK and PI3K/Akt to induce intrinsic apoptosis in a hamster model of oral cancer", *Biochimica et Biophysica Acta -General Subjects,* 1830**,** 4433-4444.

Khan, M. N., Haggag, Y. A., Lane, M. E., Mccarron, P. A. & Tambuwala, M. M. 2018, "Polymeric nano-encapsulation of curcumin enhances its anti-cancer activity in breast (MDA-MB231) and lung (A549) cancer cells through reduction in expression of HIF-1α and nuclear p65 (REL A)", *Current Drug Delivery,* 15**,** 286-295.

Kim, M. S., Ahn, Y. T., Lee, C. W., Kim, H. & An, W. G. 2020, "Astaxanthin Modulates Apoptotic Molecules to Induce Death of SKBR3 Breast Cancer Cells", *Marine Drugs,* 18**,** 266.

Leiva-Vega, J., Villalobos-Carvajal, R., Ferrari, G., Donsì, F., Zúñiga, R. N., Shene, C. & Beldarraín-Iznaga, T. 2020, "Influence of interfacial structure on physical stability and antioxidant activity of curcumin multilayer emulsions", *Food and Bioproducts Processing,* 121**,** 65-75.

Lim, S. M., Pang, Z. W., Tan, H. Y., Shaikh, M., Adinarayana, G. & Garg, S. 2015, "Enhancement of docetaxel solubility using binary and ternary solid dispersion systems", *Drug Development Industrial Pharmacy,* 41**,** 1847-1855.

Liu, A., Lou, H., Zhao, L. & Fan, P. 2006a, "Validated LC/MS/MS assay for curcumin and tetrahydrocurcumin in rat plasma and application to pharmacokinetic study of phospholipid complex of curcumin", *Journal of Pharmaceutical and Biomedical Analysis,* 40**,** 720-727.

Liu, C., Zhang, S., Mcclements, D. J., Wang, D. & Xu, Y. 2019, "Design of astaxanthin-loaded core–shell nanoparticles consisting of chitosan oligosaccharides and poly (lactic-co-glycolic acid): enhancement of water solubility, stability, and bioavailability", *Journal of Agricultural Food Chemistry,* 67**,** 5113-5121.

Liu, F., Gao, S., Yang, Y., Zhao, X., Fan, Y., Ma, W., Yang, D., Yang, A. & Yu, Y. 2017, "Curcumin induced autophagy anticancer effects on human lung adenocarcinoma cell line A549", *Oncology Letters,* 14**,** 2775-2782.

Liu, J., Tu, D., Dancey, J., Reyno, L., Pritchard, K. I., Pater, J. & Seymour, L. K. 2006b, "Quality of life analyses in a clinical trial of DPPE (tesmilifene) plus doxorubicin versus doxorubicin in patients with advanced or metastatic breast cancer: NCIC CTG Trial MA. 19", *Breast Cancer Research and Treatment,* 100**,** 263-271.

Liu, W., Zhai, Y., Heng, X., Che, F. Y., Chen, W., Sun, D. & Zhai, G. 2016a, "Oral bioavailability of curcumin: problems and advancements", *Journal of Drug Targeting,* 24**,** 694-702.

Liu, X., Song, M., Gao, Z., Cai, X., Dixon, W., Chen, X., Cao, Y., Xiao, H. 2016b, "Stereoisomers of astaxanthin inhibit human colon cancer cell growth by inducing G2/M cell cycle arrest and apoptosis", *Journal of Agricultural and Food Chemistry,* 64**,** 7750-7759.

Lockwood, S. F., O'malley, S. & Mosher, G. L. 2003, "Improved aqueous solubility of crystalline astaxanthin (3, 3′-dihydroxy-β, β-carotene-4, 4′-dione) by Captisol®(sulfobutyl ether β-cyclodextrin)", *Journal of Pharmaceutical Sciences,* 92**,** 922-926.

Madhavi, D., Kagan, D. & Seshadri, S. 2018, "A Study on the Bioavailability of a Proprietary, Sustained-release Formulation of Astaxanthin", *Integrative Medicine: A Clinician's Journal,* 17**,** 38.

Mccubrey, J. A., Lertpiriyapong, K., Steelman, L. S., Abrams, S. L., Yang, L. V., Murata, R. M., Rosalen, P. L., Scalisi, A., Neri, L. M. & Cocco, L. 2017, "Effects of resveratrol, curcumin, berberine and other nutraceuticals on aging, cancer development, cancer stem cells and microRNAs", *Aging,* 9**,** 1477.

Mcfarland, D. C. 2019, "New lung cancer treatments (immunotherapy and targeted therapies) and their associations with depression and other psychological side effects as compared to chemotherapy", *General Hospital Psychiatry,* 60**,** 148-155.

Miyashita, K., Beppu, F., Hosokawa, M., Liu, X. & Wang, S. 2020, "Nutraceutical characteristics of the brown seaweed carotenoid fucoxanthin", *Archives of Biochemistry Biophysics,* 686**,** 108364.

Mosmann, T. 1983, "Rapid colorimetric assay for cellular growth and survival: application to proliferation and cytotoxicity assays", *Journal of Immunological Methods,* 65**,** 55-63.

Münstedt, K., Momm, F. & Hübner, J. 2019, "Honey in the management of side effects of radiotherapy-or radio/chemotherapy-induced oral mucositis- A systematic review", *Complementary Therapies in Clinical Practice,* 34**,** 145-152.

Ngwabebhoh, F. A., Erdagi, S. I. & Yildiz, U. 2018, "Pickering emulsions stabilized nanocellulosic-based nanoparticles for coumarin and curcumin nanoencapsulations: In vitro release, anticancer and antimicrobial activities", *Carbohydrate Polymers,* 201**,** 317-328.

Onetto, N., Rozencweig, M. & Canetta, R. 1992, "An integrated analysis of the safety of single agent taxol. Second National Cancer Institute Workshop on Taxol and Taxus", 23-4.

Parikh, A., Kathawala, K., Song, Y., Zhou, X.-F. & Garg, S. 2018, "Curcumin-loaded self-nanomicellizing solid dispersion system: part I: development, optimization, characterization, and oral bioavailability", *Drug Delivery Translational Research,* 8**,** 1389-1405.

Pathak, L., Kanwal, A. & Agrawal, Y. 2015, "Curcumin loaded self assembled lipid-biopolymer nanoparticles for functional food applications", *Journal of Food Science Technology,* 52**,** 6143-6156.

Priyadarsini, K. I. 2009, "Photophysics, photochemistry and photobiology of curcumin: Studies from organic solutions, bio-mimetics and living cells", *Journal of Photochemistry and Photobiology C: Photochemistry Reviews,* 10**,** 81-95.

Purpura, M., Lowery, R. P., Wilson, J. M., Mannan, H., Münch, G. & Razmovski-Naumovski, V. 2018, "Analysis of different innovative formulations of curcumin for improved relative oral bioavailability in human subjects", *European journal of nutrition,* 57**,** 929-938.

Rao, A. R., Baskaran, V., Sarada, R. & Ravishankar, G. A. 2013, "In vivo bioavailability and antioxidant activity of carotenoids from microalgal biomass—A repeated dose study", *Food Research International,* 54**,** 711-717.

Rowinsky, E. K., Cazenave, L. A. & Donehower, R. C. 1990, "Taxol: a novel investigational antimicrotubule agent", *JNCI: Journal of the National Cancer Institute,* 82**,** 1247-1259.

Rowinsky, E. K., Onetto, N., Canetta, R. & Arbuck, S. 1992, "Taxol: the first of the taxanes, an important new class of antitumor agents", *Seminars in Oncology,* 646-662.

Santana-Gálvez, J., Villela-Castrejón, J., Serna-Saldívar, S. O., Cisneros-Zevallos, L. & Jacobo-Velázquez, D. A. 2020, "Synergistic Combinations of Curcumin, Sulforaphane, and Dihydrocaffeic Acid against Human Colon Cancer Cells", *International Journal of Molecular Sciences,* 21**,** 3108.

Shakibaei, M., Mobasheri, A., Lueders, C., Busch, F., Shayan, P. & Goel, A. 2013, "Curcumin enhances the effect of chemotherapy against colorectal cancer cells by inhibition of NF-κB and Src protein kinase signaling pathways", *PloS One,* 8**,** e57218.

Shanmugapriya, K., Kim, H., Saravana, P. S., Chun, B.-S. & Kang, H. W. 2018, "Astaxanthin-alpha tocopherol nanoemulsion formulation by emulsification methods: Investigation on anticancer, wound healing, and antibacterial effects", *Colloids Surfaces B: Biointerfaces,* 172**,** 170-179.

Shanmugapriya, K., Kim, H. & Kang, H. W. 2019, "In vitro antitumor potential of astaxanthin nanoemulsion against cancer cells via mitochondrial mediated apoptosis", *International Journal of Pharmaceutics,* 560**,** 334-346.

Shen, X., Fang, T., Zheng, J. & Guo, M. 2019, "Physicochemical Properties and Cellular Uptake of Astaxanthin-Loaded Emulsions", *Molecules,* 24**,** 727.

Shen, X., Zhao, C., Lu, J. & Guo, M. 2018, "Physicochemical properties of whey-protein-stabilized astaxanthin nanodispersion and its transport via a Caco-2 monolayer", *Journal of Agricultural Food Chemistry,* 66**,** 1472-1478.

Slika, L., Moubarak, A., Borjac, J., Baydoun, E., Patra, D. J. M. S. & C, E. 2020, "Preparation of curcumin-poly (allyl amine) hydrochloride based nanocapsules: Piperine in nanocapsules accelerates encapsulation and release of curcumin and effectiveness against colon cancer cells", *Material Sciences and Engineering,* 109**,** 110550.

Sun, J., Bi, C., Chan, H. M., Sun, S., Zhang, Q. & Zheng, Y. 2013, "Curcumin-loaded solid lipid nanoparticles have prolonged in vitro antitumour activity, cellular uptake and improved in vivo bioavailability", *Colloids Surfaces B: Biointerfaces,* 111**,** 367-375.

Tan, S., Li, D. & Zhu, X. 2020, "Cancer immunotherapy: Pros, cons and beyond", *Biomedicine Pharmacotherapy,* 124**,** 109821.

Thorn, C. F., Oshiro, C., Marsh, S., Hernandez-Boussard, T., Mcleod, H., Klein, T. E. & Altman, R. B. 2011, "Doxorubicin pathways: pharmacodynamics and adverse effects", *Pharmacogenetics genomics,* 21**,** 440.

Vasconcelos, T., Prezotti, F., Araújo, F., Lopes, C., Loureiro, A., Marques, S. & Sarmento, B. 2021, "Third-generation solid dispersion combining Soluplus and poloxamer 407 enhances the oral bioavailability of resveratrol", *International Journal of Pharmaceutics***,** 120245.

Vijay, K., Sowmya, P. R.-R., Arathi, B. P., Shilpa, S., Shwetha, H. J., Raju, M., Baskaran, V. & Lakshminarayana, R. 2018, "Low-dose doxorubicin with carotenoids selectively alters redox status and upregulates oxidative stress-mediated apoptosis in breast cancer cells", *Food Chemical Toxicology,* 118**,** 675-690.

Walia, N., Dasgupta, N., Ranjan, S., Ramalingam, C. & Gandhi, M. 2019, "Methods for nanoemulsion and nanoencapsulation of food bioactives", *Environmental Chemistry Letters***,** 1-13.

Walker, F. E, 1993, "Paclitaxel (TAXOL®): Side effects and patient education issues", *Seminars in oncology nursing,* 9**,** 6-10.

Wirsdörfer, F., De Leve, S. & Jendrossek, V. 2019, "Combining radiotherapy and immunotherapy in lung cancer: can we expect limitations due to altered normal tissue toxicity?", *International Journal of Molecular Sciences,* 20**,** 24.

Wulandari, F., Meiyanto, E., Kirihata, M. & Hermawan, A. 2020, "Bioinformatic analysis of CCA-1.1, a novel curcumin analog, uncovers furthermost noticeable target genes in colon cancer", *Gene Report,* 21**,** 100917.

Xiong, S., Feng, Y. & Cheng, L. 2019, "Cellular Reprogramming as a therapeutic target in cancer", *Trends in Cell Biology,* 29, 623-634.

Yallapu, M. M., Jaggi, M. & Chauhan, S. C. 2010, "β-Cyclodextrin-curcumin self-assembly enhances curcumin delivery in prostate cancer cells", *Colloids Surfaces B: Biointerfaces,* 79**,** 113-125.

Yang, L., Qiao, X., Gu, J., Li, X., Cao, Y., Xu, J. & Xue, C. 2020, "Influence of molecular structure of astaxanthin esters on their stability and bioavailability", *Food Chemistry,* 343**,** 128497.

Yang, K.-Y., Lin, L.-C., Tseng, T.-Y., Wang, S.-C. & Tsai, T.-H. 2007, "Oral bioavailability of curcumin in rat and the herbal analysis from Curcuma longa by LC–MS/MS", *Journal of Chromatography B,* 853**,** 183-189.

Yang, R., Wei, T., Goldberg, H., Wang, W., Cullion, K. & Kohane, D. S. 2017, "Getting drugs across biological barriers", *Advanced Materials,* 29**,** 1606596.

Yuan, C., Jin, Z. & Xu, X. 2012, "Inclusion complex of astaxanthin with hydroxypropyl-β-cyclodextrin: UV, FTIR, 1H NMR and molecular modeling studies", *Carbohydrate polymers,* 89**,** 492-496.

Zanoni, F., Vakarelova, M. & Zoccatelli, G. 2019, “Development and Characterization of Astaxanthin-Containing Whey Protein-Based Nanoparticles”, *Marine Drugs*, 17**,** 627.

Zhang, D., Wang, J. & Xu, D. 2016, “Cell-penetrating peptides as noninvasive transmembrane vectors for the development of novel multifunctional drug-delivery systems”, *Journal of Controlled Release*, 229**,** 130-139.

Zhang, X., Yin, W., Qi, Y., Li, X., Zhang, W. & He, G. 2017, “Microencapsulation of astaxanthin in alginate using modified emulsion technology: Preparation, characterization, and cytostatic activity”, *The Canadian Journal of Chemical Engineering,* 95**,** 412-419.

Zi, P., Zhang, C., Ju, C., Su, Z., Bao, Y., Gao, J., Sun, J., Lu, J. & Zhang, C. 2019, "Solubility and bioavailability enhancement study of lopinavir solid dispersion matrixed with a polymeric surfactant-Soluplus", *European Journal of Pharmaceutical Sciences*, 134**,** 233-245.

Appendix

1. FTIR spectra analysis of SOL

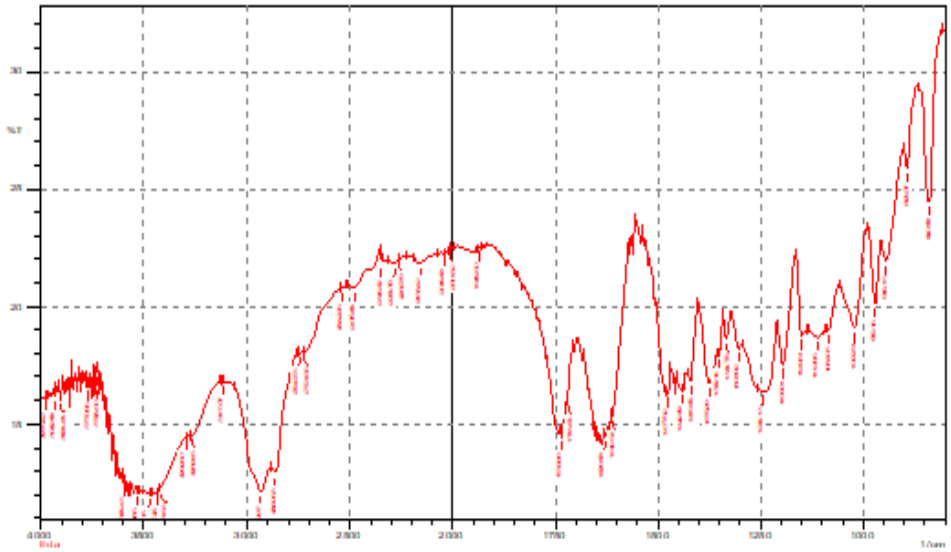

2. Standard curve of AST

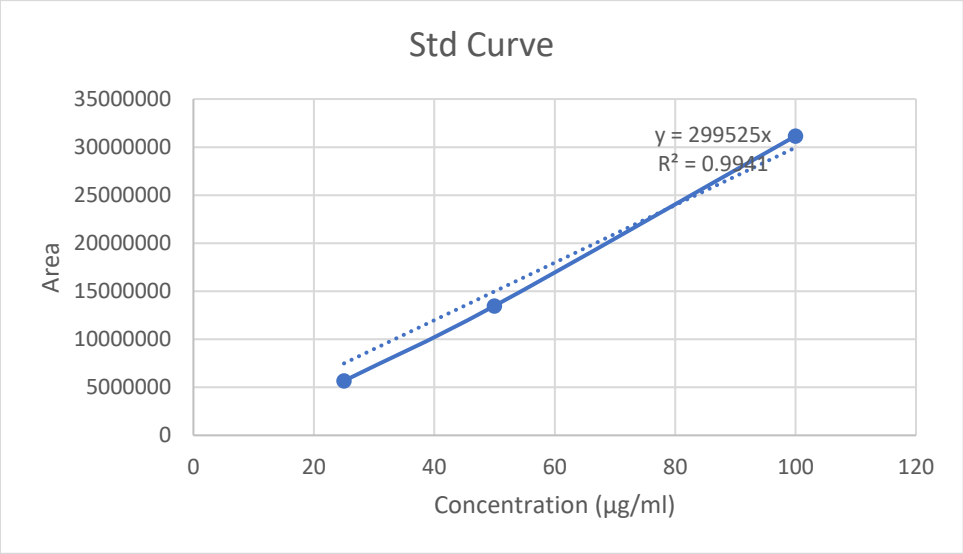

3. Standard curve of CUR

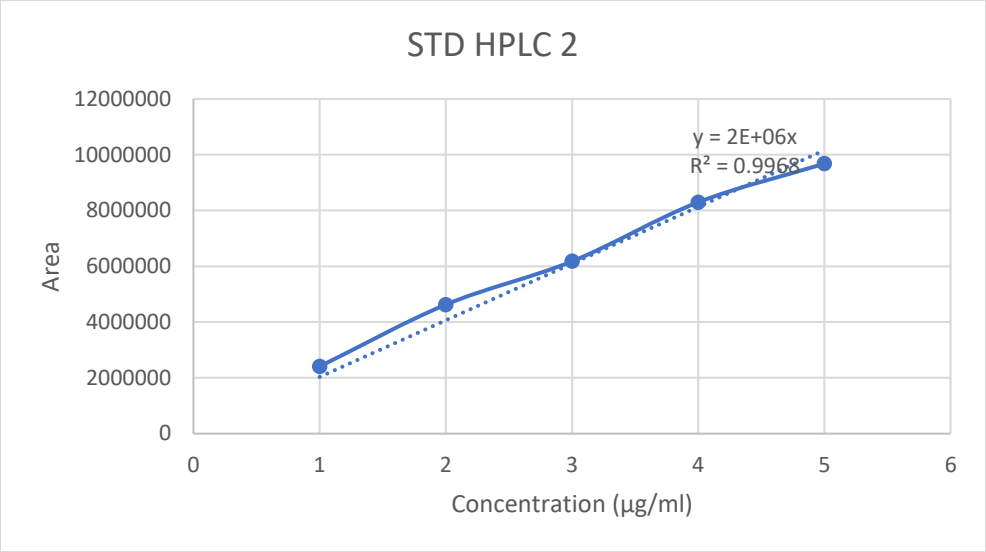

4. DSC of SOL

4. Images of compounds dissolved in 1 ml water and DMSO respectively.

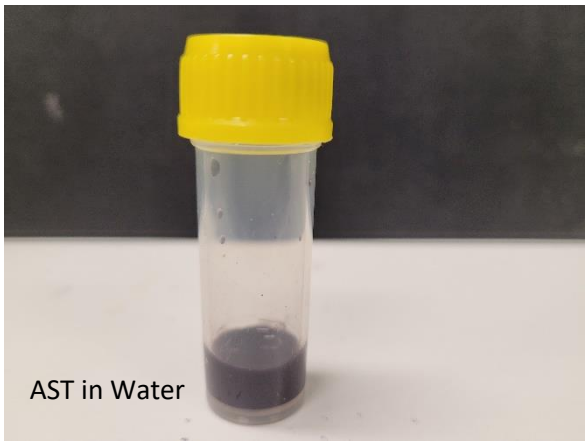

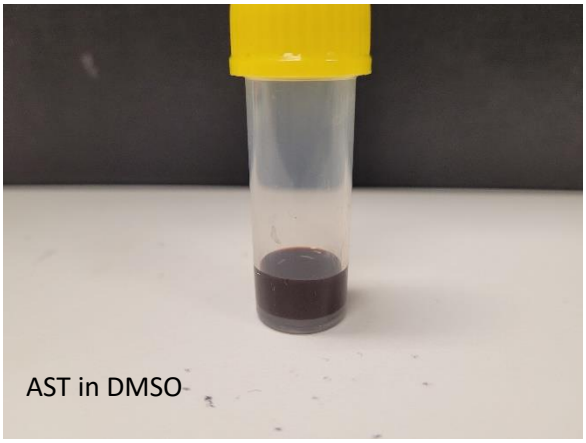

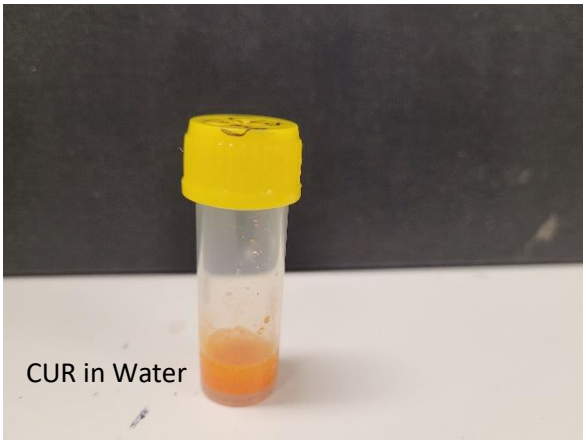

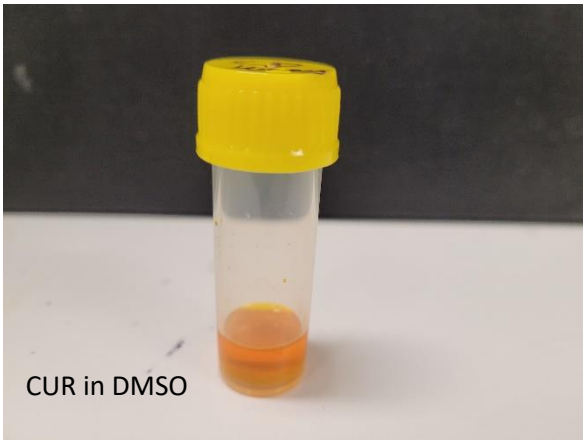

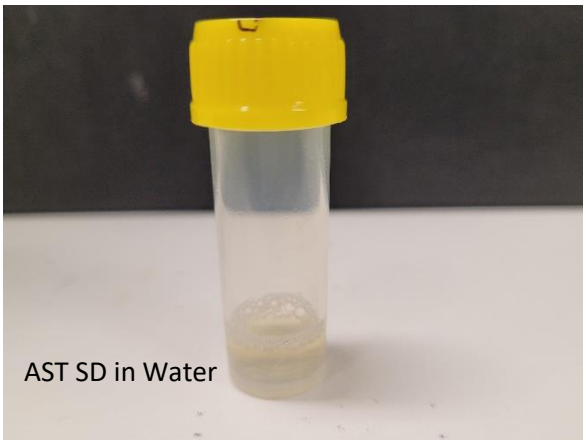

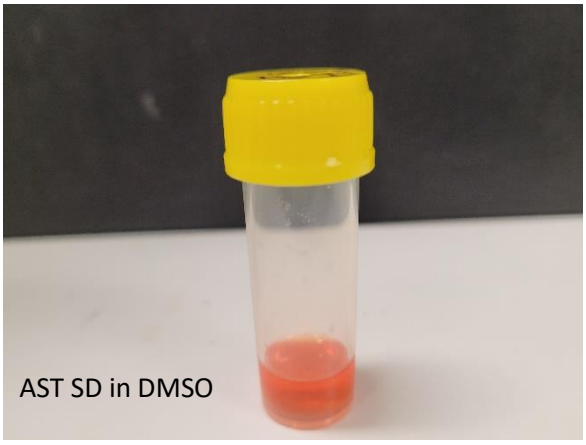

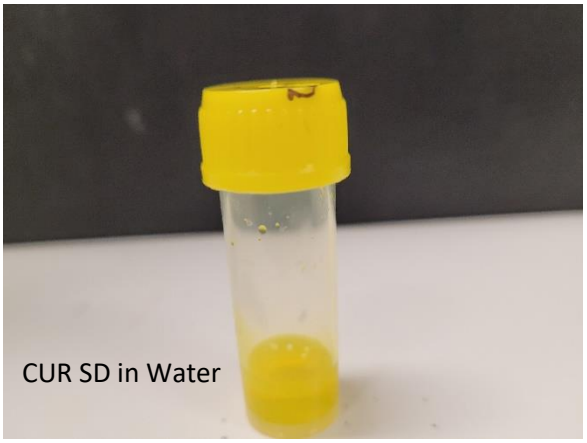
CUR SD in Water

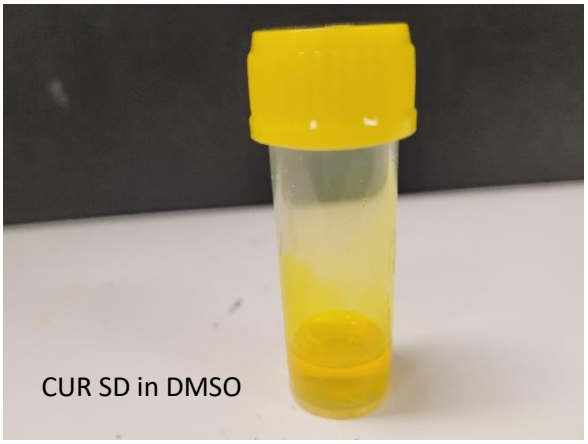
CUR SD in DMSO

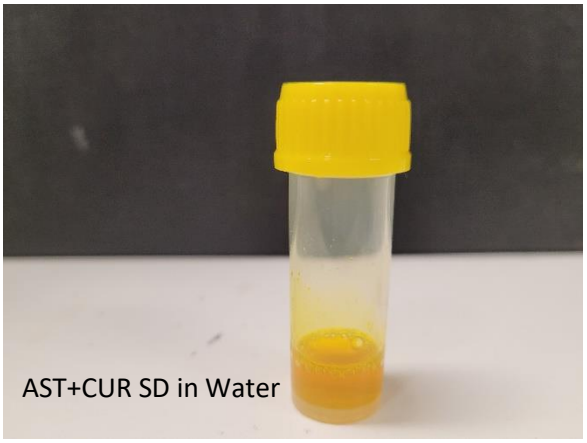
AST+CUR SD in Water

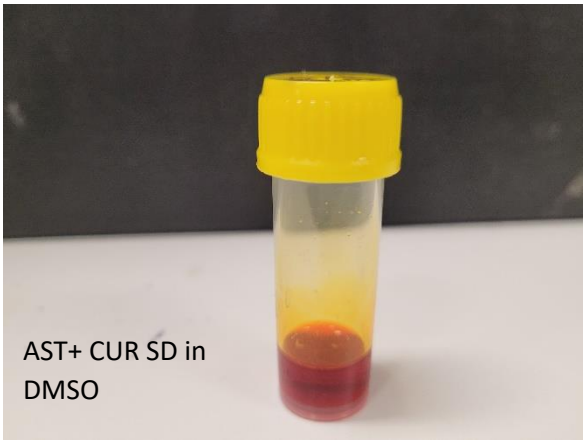
AST+ CUR SD in
DMSO